



Programme

9:00 Arrival, registration, tea & coffee

9:40 Welcoming remarks (Dr Susan Currie)

Session 1- Chair: Dr Susan Currie

9:45 Keynote Lecture
Professor Keith Oldroyd, Consultant Interventional Cardiologist, Golden Jubilee Hospital, Glasgow

Coronary heart disease: physiology beats anatomy

10:30 O1: **Urinary proteomics can be predictive of cardiovascular events.**
Catriona Brown, University Of Glasgow

10:45 O2: ***In vivo* cardiac cine ²³Na MRI in rats.**
Maurits A Jansen, University Of Edinburgh

11:00 Tea, coffee, exhibits & posters

11:30 O3: **Global protein palmitoylation mapping in cardiac muscle.**
Louise Reilly, University Of Dundee

11:45 O4: **Arrhythmogenesis in heart failure – effect of exercise training.**
Olivia Robertson-Gray, University Of Glasgow

12:00 O5: **Intermedin protects against ischaemia and reperfusion injury in human ventricular cardiomyocytes: receptor subtype involvement.**
Stephen F. McAleer, Queen's University Belfast

12:15 O6: **Characterisation of cardiomyocytes derived from human induced pluripotent stem (iPS) cells.**
Franziska Sendfeld, University Of Edinburgh.

12:30 Lunch, posters & exhibits

13:00 SCF Committee Meeting

Session 2- Chair: Dr Hilary Carswell

14:15 O7: **Cavin-1: a novel regulator of the SOCS3 E3 ubiquitin ligase.**

Jamie J. L. Williams, University Of Glasgow

14:30 O8: **Androgen receptors regulate vascular remodelling following arterial injury**

Junxi Wu, University Of Edinburgh

14:45 O9: **Vascular smooth muscle proliferation is inhibited by impeding the switch from a stationary to a motile mitochondrial phenotype.**

Susan Chalmers, University Of Strathclyde

15:00 O10: **Effects of chronic dietary intervention and post-prandial effects on circulating cell-derived microparticle concentrations in type 2 diabetes.**

Xuguang Zhang, University Of Aberdeen

15:15 Tea, coffee, posters & exhibits

15:30 O11: **Human serum microRNA profiles after ischaemic stroke.**

Christopher R Breen, University Of Glasgow

15:45 O12: **Mast cell dependent pathology may be mediated by endothelin-1, matrixmetalloproteinase-9 and endoglin after transient middle cerebral artery occlusion.**

Craig McKittrick, University Of Strathclyde.

16:00 Keynote Lecture

Professor I. Mhairi Macrae, Professor of Neuroscience, University of Glasgow

A new spin on stroke research: using MRI to investigate new therapies

16:45 SCF Announcements & Prizes

Professor Cherry Wainwright, Institute for Health & Welfare Research, Robert Gordon University, Aberdeen

17:00 Meeting Closes

LIST OF POSTER COMMUNICATIONS:

- P1 **Syed.** Characterisation of signalling mechanisms that underlie P2Y receptor-mediated vasoconstriction of rat intrapulmonary artery
- P2 **Baird.** B-vitamin deficiency, gene expression and DNA methylation in vascular smooth muscle cells
- P3 **Ahmad.** Anti-hypertensive Effects of the Aqueous and Its Residual Methanolic Extracts of *Syzygium polyanthum* Wight. Walp. Var. *Polyanthum* Leaves
- P4 **Yeong.** Adherence to Heart Failure Therapy and Outcome: A Population Based Study
- P5 **Johnston.** Post-myocardial infarction exercise training reverses cardiac excitation-contraction coupling abnormalities by activating cytoplasmic CAMKII
- P6 **Halliday.** The Role of microRNA 21 in Porcine and Murine Models of In-Stent Restenosis
- P7 **Huesa.** Quantitative 3-dimensional imaging of aortic calcification by micro computed tomography
- P8 **Yarham.** Identification of microRNA target sites in $K_{ir}2.1$ 3' UTR by a novel dual-fluorescent assay
- P9 **MacAskill.** Development of a rabbit model of arteriovenous fistula remodelling
- P10 **Hadoke.** Selective smooth muscle cell ETB receptor deletion abolishes sarafotoxin 6c-mediated vasoconstriction
- P11 **Henry.** Spontaneous Ca^{2+} transients in rat pulmonary vein cardiomyocytes following electrical field stimulation
- P12 **Lappin.** GPR35 as a novel therapeutic target of cardiovascular disease
- P13 **Syed.** Comparison of the agonist activities of treprostinil and naxaprostene in systemic blood vessels
- P14 **Akbar.** MAPKAP 2/3: a novel target to sequester cholesterol induced cardiovascular diseases *in vivo*?
- P15 **Brown.** Sudden death referrals to the West of Scotland Inherited Cardiac Conditions Clinic: an overview
- P16 **McCormick** Drug Delivery from Coronary Stents: insights from mathematical models
- P17 **Docherty.** Distribution and expression pattern of the cardiac slow delayed rectifier channel in the human heart
- P18 **Crawford.** Identification and functional validation of osteopontin as a candidate gene for left ventricular mass index in the stroke prone – spontaneously hypertensive rat
- P19 **Daly** Distinctive profile of isomiR expression and novel microRNAs in rat heart left ventricle

- P20 **Dashti.** A combined approach on integrated functional genomics data to prioritize candidate genes in the stroke-prone spontaneously hypertensive and wistar kyoto rats
- P21 **Cassidy.** Myocardial Fat in Cardiovascular Disease; A Diabetic Perspective
- P22 **Emerson.** Expression and localisation of H₂S metabolising enzymes in the murine myocardium and liver
- P23 **Ford.** Evaluation of laboratory tests for aspirin response in patients with stable cardiovascular disease
- P24 **Carr.** MitoSNO1 as a potential therapeutic in experimental stroke
- P25 **Kokkalis.** Comparing the haemodynamic differences in the outflow of vascular prostheses
- P26 **Mair.** Beneficial effects of an aromatase inhibitor in two distinct models of established pulmonary arterial hypertension.
- P27 **Maskrey.** Aspirin-induced inhibition of platelet aggregation and eicosanoid metabolism: more than just an inhibitor of cyclooxygenase?
- P28 **Matthew.** High variability in peak signal intensity and contrast dynamics during first pass perfusion imaging: a CMRI study
- P29 **McCormick.** Intra and inter-observer variability in whole-body contrast enhanced MRA stenosis grading and systemic atheroma scoring
- P30 **McDonald.** MicroRNA analysis in experimental models of vein graft neointima formation identifies a critical role for miR-21 in neointima formation.
- P31 **Ord.** A combined gene-therapy and pharmacological intervention protects from cerebral ischaemia *in vivo* and hypoxia / reoxygenation *in vitro*.
- P32 **Reis.** Lipidome profile of human LDL: finding out the best extraction solvent system
- P33 **Hutchison.** The Role of Sodium Channels Present on the Rat Pulmonary Vein in the Generation of Arrhythmogenic Activity in Atrial Fibrillation
- P34 **Al-Dujali.** Polyphenol-rich foods intake reduces CVD risk factors in healthy volunteers.
- P35 **Lockhart.** GLP-1 peptides attenuate agonist-induced hypertrophy in H9c2 cardiomyocytes
- P36 **Hamilton.** Sex differences in vascular endothelial cell function reveal a gender specific role for nitroxyl
- P37 **Gray.** Imaging the healing murine myocardial infarct *in vivo*: ultrasound, MRI and fluorescence molecular tomography.
- P38 **Richardson.** Glucocorticoid receptor deficiency in cardiomyocytes results in cardiac fibrosis in adult mice
- P39 **Martin.** Effects of bs906, anHSP20-PDE4 disruptor, on hypertrophic remodelling *in vivo*

- P40 **Campbell.** The Role of Intermedin in modulating functional changes associated with Pulmonary Hypertension
- P41 **Semaan.** Finding potential anti-diabetic compounds from *Allophylus cominia Sw.*
- P42 **Stevenson.** Pharmacological analysis of sympathetically-mediated constriction in mouse tail artery
- P43 **Stott.** Pulmonary exposure to diesel exhaust particulate inhibits the cytoprotective mechanisms of the heart
- P44 **Syed.** Differences in the signalling mechanisms underlying UTP-evoked vasoconstriction of pulmonary and systemic-like arteries
- P45 **Torrance.** A critical role for MAP kinase phosphatase-2 in the completion of vascular smooth muscle cell cytokinesis
- P46 **van Kralingen.** Canine adenovirus as a novel gene delivery vector for experimental stroke studies.
- P47 **Rosli.** Pharmacological effects of gallic acid from *benincasa hispida* prepared with different extraction techniques: a preliminary quantitative analysis
- P48 **White.** Cardiovascular phenotyping of mice with targeted 11 β -hydroxysteroid dehydrogenase type 1 deletion
- P49 **White.** The miR-143/145 cluster is dysregulated during progression of vein graft and in-stent neointima formation but genetic deletion in mice does not influence lesion formation.
- P50 **Wilson.** Glucocorticoids are important for maturation and development of the zebrafish embryo cardiovascular system.
- P51 **Zhu.** A protective role for FGF23 in local defence against disrupted arterial wall integrity?

ABSTRACTS FOR ORAL COMMUNICATIONS

O1

Urinary proteomics can be predictive of cardiovascular events

Catriona Brown¹, Harald Mischak¹, Amaya Abalat¹, William Mullen¹, Naveed Sattar¹, Nina S McCarthy², Alun D Hughes³, Simon Thom³, Jamil Mayet³, Alice Stanton², Peter Sever³, Anna F Dominiczak¹, Christian Delles¹

¹ *Institute of Cardiovascular and Medical Sciences, University of Glasgow, UK*

² *Royal College of Surgeons in Ireland Medical School, Dublin, Ireland*

³ *Imperial College London, UK*

OBJECTIVES. We have previously demonstrated associations between the urinary proteome profile and coronary artery disease (CAD) in cross-sectional studies. Here we evaluated the potential of urinary proteomics as a predictor of CAD in the "Hypertension Associated Cardiovascular Disease" (HACVD) sub-study population of the ASCOT study.

DESIGN AND METHODS. Thirty-seven cases with the primary endpoint CAD (fatal CAD, symptomatic non-fatal myocardial infarction and coronary revascularisation) were selected and matched for sex and age within +/-2 years to controls who had not reached a CAD endpoint during the study (median observation time, 5 years). Study participants with established cardiovascular disease at baseline were not included. A spot urine sample collected at 1 to 1.5 years post randomisation was analysed using capillary electrophoresis (CE) on-line coupled to Micro-TOF mass spectrometry (MS). The previously developed CE-MS model for CAD and three unrelated models (chronic kidney disease, CKD; heart failure, HF; stroke) were assessed for their predictive values, and a classifier was calculated for each sample for each model.

RESULTS. Sixty urine samples (32 cases; 28 controls; 88% male, mean age 64±5 years) passed quality control for proteomic analysis. As expected, classifiers were not different between cases and controls respectively for the CKD (-0.069±0.388 vs -0.095±0.236, $P=0.752$), HF (0.282±0.663 vs 0.114± 0.569, $P=0.301$) and stroke models (-0.114±0.679 vs -0.140±0.528, $P=0.868$). In contrast, there was a trend towards lower ("healthier") values in controls for the CAD model (-0.432±0.326 vs -0.587±0.297, $P=0.062$), and the CAD model showed statistical significance on Kaplan-Meier survival analysis (Log Rank (Mantel-Cox) $P=0.021$).

CONCLUSIONS. Due to its limited sample size this proof-of-concept study cannot evaluate the additive predictive value of proteomics compared to other traditional risk factors including lipids and diabetes. We have, however, shown that a CAD specific urinary proteome panel that was developed in a cross-sectional study predicts CAD endpoints independent of age and sex in a well controlled prospective study, indicating that urinary proteomics should be tested for its predictive potential in cardiovascular risk assessment.

O2

In vivo cardiac cine ^{23}Na MRI in rats

Maurits A Jansen^{1,2}, Urte Kägebein^{1,2}, Gillian A Gray², Friedrich Wetterling³, Ian Marshall^{1,2}

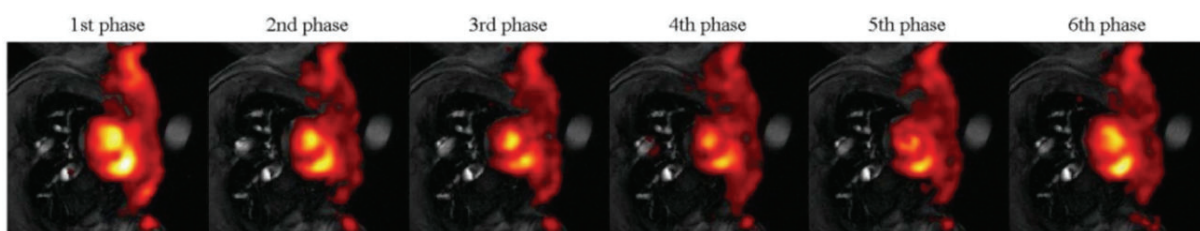
¹Edinburgh Preclinical Imaging ²University and British Heart Foundation Centre for Cardiovascular Science, University of Edinburgh ³Faculty of Engineering, Trinity College Dublin, Ireland

Background. Absolute tissue sodium concentration is elevated in myocardial infarction and has been suggested as a biomarker for cell viability. Sodium MRI is challenging due to relatively low sodium concentrations in biological tissues, low NMR sensitivity and the short T2 of ^{23}Na . Untriggered ^{23}Na chemical shift imaging (CSI) was previously used for imaging of isolated perfused rat hearts (Jansen et al., *Circulation* 2004, 110(22)). For imaging of the *in vivo* heart, however, ECG-triggering is required to minimize image blurring due to cardiac motion, which poses restrictions on the repetition time (TR).

Objectives. To implement and test a new ^{23}Na chemical shift imaging method for imaging of the *in vivo* rat heart during several different phases of the cardiac cycle with sufficient spatial resolution.

Methods. Rats (n=6) were scanned in a 7T MRI scanner. ECG-triggered cine ^1H MRI was performed for functional assessment and anatomical reference. ECG-triggered 2D ^{23}Na CSI images were acquired with a 1-mm in plane resolution and 3.5 mm slice thickness, either at only 1 phase during the cardiac cycle (end-diastolic or end-systolic) or up to 6 phases (cine version, effective TR 30 ms) equally distributed over the cardiac cycle in ~70 min.

Results. The myocardium as well as the left and right ventricle of the heart were clearly visible (figure, ^{23}Na (colour) overlaid on ^1H image (B&W)). The ^{23}Na myocardium/blood signal ratio was 0.46 ± 0.05 , which is in good agreement with the reported value of 0.45. Using the cine version of the CSI sequence, up to 6 frames of the cardiac cycle could be recorded with reduced TR (~30ms) but similar image quality (myocardium/blood signal ratio: 0.44 ± 0.07).



Discussion and conclusions. To our knowledge, these are the first reported *in vivo* rat cardiac ^{23}Na MR images. The CSI sequence can be used to acquire one or several phases during the cardiac cycle as shown above, but also to cover multiple slices through the heart. When used in combination with a ^{23}Na shift reagent, the sequence potentially allows for discrimination of intra- and extracellular Na signals, because the frequency information is preserved as opposed to other types of MRI sequences like ultra-short TE. This method offers a new tool for studying myocardial ion homeostasis *in vivo* and may be of interest for different areas of cardiovascular disease, e.g. myocardial infarction, myocardial hypertrophy, but could also be used to study other organs like kidney, liver or tumours.

03

Global protein palmitoylation mapping in cardiac muscle.

L Reilly¹, M Ashford¹, W Fuller¹

1: Division of Cardiovascular and Diabetes Medicine, Medical Research Institute, University of Dundee

The palmitoyl proteome in cardiac tissue remains largely uncharacterised. Only a few proteins have been identified as palmitoylated, for example the sodium pump regulator phospholemman. Given that palmitoylation regulates ion channels and transporters, it may be as important as phosphorylation in the regulation of excitation-contraction coupling and thus cardiac output. Using resin assisted capture (acyl rac), we enriched palmitoylated proteins from rat ventricular myocytes. Cysteine residues were differentially alkylated to distinguish between palmitoylated and non-palmitoylated residues. Resultant proteins were digested and identified by LC-MS/MS. Approximately 1000 proteins were identified from 3 independent experiments. Mitochondrial proteins were eliminated using the MitoMiner database. Functional clustering of the remaining proteins revealed multiple functional groups including glycolytic enzymes, G proteins and ion transporters are palmitoylated in ventricular myocytes. The addition of lipid anchors to glycolytic enzymes raises the possibility that glycolysis may be compartmentalised to specific subcellular locations in cardiac muscle. The protein acyl transferases (PATs) DHHC5, DHHC7 and DHHC23 were also found expressed and palmitoylated in ventricular myocytes. The palmitoylation sites of both these enzymes were multiple cysteines in the cysteine rich domain upstream of the DHHC motif, although notably only one cysteine per PAT was ever found palmitoylated. This data highlights previously unknown palmitoylated proteins in cardiac tissue. Given PATs are palmitoylated with a stoichiometry of <1 molecule of palmitate per PAT, their palmitoylation upstream of the DHHC motif offers insight into their enzymatic mechanism.

O4

Arrhythmogenesis in Heart Failure – Effect of Exercise Training

Olivia Robertson-Gray, Michael Dunne, Ole J. Kemi

University of Glasgow, Glasgow, UK

Left ventricle (LV) arrhythmogenesis is increased in heart failure, of which some events are linked to abnormalities in excitation-contraction coupling (ECC) including modulation via Ca^{2+} /calmodulin-dependent protein kinase II (CaMKII). Exercise has contractile benefits but it remains unknown whether it may also reduce arrhythmias. Therefore, this study examined the effects that exercise training (ET) had on ventricular fibrillation (VF) susceptibility in isolated rat hearts. Rats were randomised into the following groups: control (sedentary), myocardial infarction (MI) (sedentary) and MI (training) where MI was induced by permanent coronary artery ligation. Training involved a ten minute warm-up period followed by 5 minute intervals of high intensity exercise (85-90% VO_{2max}) interrupted with 3 minute recovery periods (50% VO_{2max}) for one hour, five times a week. Each heart was removed, isolated and Langendorff-perfused at physiological conditions. Subsequently, the LV was paced whilst increasing electrical current was delivered to the right ventricle (RV) via burst stimulation. The current at which VF was induced denoted the threshold. Studies were subsequently conducted in the presence of autocalcitrin 2-related inhibitory peptide II (AIP), a CaMKII inhibitor. MI (sedentary) and MI (training) hearts were significantly more susceptible to VF compared to the control (sedentary) hearts ($P < 0.01$). ET did not alter the VF threshold amongst groups. Additionally, the VF threshold was significantly reduced in the presence of AIP in hearts from the control (sedentary) group ($P < 0.01$) whereas no difference in VF threshold was observed in the MI (sedentary) or MI (training) hearts in the presence of this inhibitor. In conclusion, isolated rat hearts are more susceptible to VF post MI regardless of ET. CaMKII plays a protective role in health but does not alter VF susceptibility post MI, regardless of exercise state

O5

Intermedin protects against Ischaemia and Reperfusion Injury in Human Ventricular Cardiomyocytes: Receptor Subtype Involvement

SF McAleer, MT Harbinson, M Ferguson, M Campbell, D Bell

School of Medicine, Dentistry and Biomedical Sciences, Queen's University Belfast, Northern Ireland, UK.

Background: Early reperfusion following myocardial infarction is essential but results in ischaemia/reperfusion (I/R) injury, whereby myocardial cells die largely due to oxidative stress. Intermedin (IMD; adrenomedullin-2), a novel peptide related to adrenomedullin (AM), is up-regulated in cardiovascular disease and is protective against I/R injury in rodent hearts and human coronary microvascular endothelial cells and cardiac non-myocytes. Protection is dependent on calcitonin receptor-like receptor (CRLR) signalling in association with one of three receptor activity-modifying proteins (RAMPs). IMD has yet to be investigated in human cardiomyocytes for a cardioprotective role.

Aims: to identify if IMD and its receptor components are expressed in human ventricular cardiomyocytes; to investigate whether IMD protects these cells against simulated I/R injury and if so, determine receptor subtype involvement.

Methods: Left ventricular adult human cardiomyocytes (HCM) were grown using normal tissue culture techniques and cells subjected to normoxia or simulated ischaemia for 4 h or I/R (3 h normoxia followed by 1 h reperfusion) all in the absence or presence of IMD. Cell viability was assessed using Trypan blue dye exclusion and oxidative damage by commercial Oxyblot assay. mRNA expression and protein distribution of IMD, AM, CRLR and RAMPs1-3 were assessed by Quantitative Real-Time PCR and indirect immunofluorescence microscopy, respectively. The silencing of the peptides or their receptor components using siRNA knock-down was employed to determine endogenous peptide and receptor subtype involvement in protection against I/R.

Results: IMD, AM and their receptor component mRNAs were expressed in HCM; RAMP2 was the most abundant RAMP, while IMD was less abundantly expressed than AM. Ischaemia or I/R reduced the HCM cell count by 40% and 60% respectively ($p < 0.05$ for both). IMD (10^{-9} mol.L⁻¹) protected against the deleterious effects of ischaemia and I/R injury (~20% salvaged for both conditions, $p < 0.05$), with preservation of cell structure when examined by phase contrast microscopy and decreased oxidative stress noted on Oxyblot ($p < 0.001$ vs. non-IMD counterpart for ischaemia or I/R). Protection was greatest when IMD was given during reperfusion ($p < 0.001$) and was abolished by silencing CRLR ($p < 0.05$) and RAMP2 ($p < 0.001$). However, silencing endogenous IMD and/or AM expression did not augment extent of I/R injury in HCM.

Conclusion: Exogenous IMD exerts a protective effect against I/R in HCM particularly during reperfusion, attributed to AM₁ receptor subtype involvement. IMD administration during cardiac reperfusion could improve levels of morbidity and mortality in patients following myocardial infarction. However, inability to demonstrate a protective effect of the endogenous peptides argues for a paracrine influence derived from alternative cardiac cell-types rather than autocrine signalling by HCM themselves.

06

Characterisation of Cardiomyocytes Derived from Human Induced Pluripotent Stem (iPS) Cells

F. Sendfeld¹, O. Tura¹, C.N. Medine¹, F. Scornik², G. Pérez², M. A. Denvir³, I. Wilmut¹, N.L. Mills¹.

1: MRC Scottish Centre for Regenerative Medicine, University of Edinburgh, UK

2: Cardiovascular Genetics Center, UdG-IdIBGi, University of Girona, Girona, Spain

3: BHF/University Centre for Cardiovascular Science, Edinburgh University, UK

Objectives: To develop an efficient method for deriving cardiomyocytes from human induced pluripotent stem (iPS) cells to study inherited cardiac channelopathies. Dermal fibroblasts from patients with cardiovascular disease can be reprogrammed to iPS cells and differentiated into cardiomyocytes that have the patient's exact genetic background. Whilst this technique has enormous potential to model inherited channelopathies, such as Brugada Syndrome, the derived cells have not been fully characterised and compared to foetal and adult cardiomyocytes.

Methods: Human embryonic stem (ES) cells and iPS cells obtained from healthy controls were differentiated into cardiomyocytes using an unguided differentiation protocol. Embroid bodies from undifferentiated ES and iPS cells were cultured for 4 days and plated onto 0.1% gelatin. Beating clusters were characterised using immunocytochemistry, RT-PCR, edge detection and electrophysiology. Derived cardiac cells were then compared to primary cardiomyocytes isolated from human foetal and adult cardiac tissue.

Results: ES and iPS derived cardiomyocytes express a wide range of cardiac markers such as GATA-4, α -actinin and troponin I. They express TTX resistant voltage dependent sodium channels and exhibit action potential triggered Ca^{2+} -induced- Ca^{2+} -release. Spontaneous contraction was observed in derived cardiomyocytes and immature human foetal cardiomyocytes.

Conclusion: Although cardiomyocytes generated from iPS cells are immature, they express typical cardiac proteins and have functional cardiac sodium channels. This differentiation system may be utilised to investigate patients with and without known genetic mutations to provide a better understanding of the pathophysiology of inherited cardiac channelopathies.

07

Cavin-1: a Novel Regulator of the SOCS3 E3 Ubiquitin Ligase

Jamie J. L. Williams¹, George S. Baillie¹, William Mullen¹, Richard Burchmore¹, Paul F. Pilch², Timothy M. Palmer¹

1: Institute of Cardiovascular and Medical Sciences, University of Glasgow

2: Boston University School of Medicine, Boston, Massachusetts, U.S.A.

Suppressor of cytokine signalling 3 (SOCS3) is an inducible specificity factor for a multi-subunit E3 ubiquitin ligase that blocks inflammatory and remodeling processes in the vasculature. Consequently approaches that enhance SOCS3 function have the potential to block vascular smooth muscle cell migration and proliferation as well as inhibit endothelial inflammation responsible for the development of many cardiovascular diseases. However the spectrum of proteins capable of interacting with SOCS3 to regulate its function remains incomplete. To address this, we performed a SILAC-facilitated comparison of tandem affinity purified ubiquitinomes from WT and SOCS3-null cells, with the aim of identifying new proteins whose ubiquitylation status is controlled by SOCS3. Using this approach we have identified cavin-1/PTRF as a protein whose ubiquitylation is significantly enhanced by SOCS3. Importantly, studies of endogenous cavin-1 expressed in adipocytes, in which SOCS3 can be induced by multiple stimuli, have shown it to be ubiquitylated.

Co-immunoprecipitation experiments and overlapping peptide array overlays demonstrated that SOCS3 interacts directly with two distinct regions within cavin-1 in an interaction that did not require tyrosine phosphorylation. Using a known SOCS3 substrate FAK1 as a control, we also demonstrate that while cavin-1 ubiquitylation is enhanced by SOCS3, it is not a substrate for the complex. Instead, SOCS3 binding to cavin-1 appears to stabilise its ubiquitylation by alternative E3 ligases. In summary, our data suggest a potentially novel role for SOCS3 in regulating caveolae assembly via binding to cavin-1, thus indirectly increasing its ubiquitylation

08

Androgen receptors regulate vascular remodelling following arterial injury

Junxi Wu^{1,2}, Iris Mair¹, Patrick WF Hadoke¹, Martin A Denvir and Lee B Smith².

BHF/ University Centre for Cardiovascular Science, and MRC Centre for Reproductive Health, University of Edinburgh, Scotland, UK.

Aims: It is well established that gender influences the development of cardiovascular disease, with men at significantly higher risk than (pre-menopausal) women. However, accumulating evidence suggests physiological levels of androgens are actually beneficial for cardiovascular disease, at least in men. It is not clear, however, whether this protective action is mediated by direct stimulation of androgen receptors (AR) or requires conversion of androgens to oestrogens. The current study addressed the hypothesis that stimulation of AR in the arterial wall influences the development of vascular diseases.

Methods and results: Adult, male C57Bl6 mice underwent orchidectomy and were allowed to recover (1 week). Femoral artery injury was then performed using intra-luminal (wire injury) and extra-luminal (ligation) procedures and the mice received either androgen replacement therapy or vehicle via subcutaneous osmotic minipump for 3 weeks.

Androgen receptors were strongly expressed in injured arteries from mice undergoing androgen replacement therapy, but weak in the vehicle control group. Androgen replacement did not alter neointimal lesion formation following wire injury but significantly improved lower limb perfusion following femoral artery ligation. To further investigate the role of vascular AR in androgen-dependent effects in arterial injury, smooth muscle-specific and endothelial specific AR knockout mouse strains have been generated using the cre-lox system. Femoral arteries from smooth muscle-specific AR knockout mice showed significant defects in vasomotor function when assessed *ex vivo*.

Summary: Our data demonstrated basal AR expression in healthy vessels. Androgen administration promoted androgen receptor expression in injured arteries and improved lower limb perfusion following ischemia. The generation of mice with selective deletion of vascular AR has confirmed that these receptors influence arterial function. These mice will be useful for clarifying the role of AR in the endothelium and smooth muscle in regulating lesion formation and angiogenesis.

09

Vascular smooth muscle proliferation is inhibited by impeding the switch from a stationary to a motile mitochondrial phenotype.

Susan Chalmers¹, Christopher Saunter², Calum Wilson¹, Marnie L. Olson¹, Paul Coats¹, John M. Girkin² and John G. McCarron¹

1: Strathclyde Institute of Pharmacy and Biomedical Sciences, University of Strathclyde, SIPBS Building, 161 Cathedral Street, Glasgow G4 0RE, UK.

2: Centre for Advanced Instrumentation, Department of Physics, Durham University, South Road, Durham, DH1 3LE, UK

Mitochondria not only provide the cell with an efficient source of ATP, but also modulate cellular Ca²⁺ signals, ROS production, redox status and lipid generation. They influence cell function in both a cell-wide manner and in microdomains, e.g. at the mouth of inositol-trisphosphate sensitive Ca²⁺ release channels to facilitate Ca²⁺ puff formation. Mitochondria are commonly described as being highly dynamic organelles that undergo extensive division and fusion and whose movement is thought to be vital for cell function. In various native cells however, including those of heart and smooth muscle, mitochondria are stationary and rigidly structured. The significance of the differences in mitochondrial behaviour to physiological function is unclear and was studied here in single myocytes and in *ex-vivo* intact resistance-sized cerebral arteries maintained at physiological pressure. We hypothesized that mitochondrial dynamics is controlled by the proliferative status of the cells.

High speed fluorescence imaging of mitochondria in live vascular smooth muscle cells shows that the organelle undergoes significant re-organisation as cells become proliferative. In non-proliferative cells mitochondria are individual (~2 µm by 0.5 µm), stationary, randomly-dispersed structures. However on entering the proliferative state mitochondria take on a more diverse architecture and become small spheres, short rod shapes, long filamentous entities and networks. When cells are proliferating mitochondria continuously move and change shape, utilising the cell's microtubular network, often shuttling back-and-forth and even sometimes transferring between cells. In the intact pressurised resistance artery mitochondria were largely immobile structures except in a small number of cells in which motility occurred. When proliferation of smooth muscle was encouraged in the intact resistance artery, in organ culture, the majority of mitochondria became motile and the majority of smooth muscle cells contained moving mitochondria. Significantly, restriction of mitochondrial motility using the inhibitor of the mitochondrial fission process Mdivi-1, inhibited vascular smooth muscle proliferation in both single cells and in the intact resistance artery.

These results show that mitochondria are adaptable and exist in intact tissue as both stationary and highly dynamic entities. This mitochondrial plasticity is an essential mechanism for the development of smooth muscle proliferation and therefore presents a novel therapeutic target against vascular disease.

O10

Effects of chronic dietary intervention and post-prandial effects on circulating cell-derived microparticle concentrations in Type 2 diabetes

X. Zhang^{1,2}, Susan C McGeoch³, Ian L Megson⁴, Sandra M MacRury⁴, Alexandra M Johnstone¹, Prakash Abraham³, Donald WM Pearson³, Grietje Holtrop⁵, Niamh O'Kennedy² & Gerald E Lobley¹

1: University of Aberdeen, Rowett Institute of Nutrition & Health, Aberdeen, UK

2: Provexis plc at the Rowett Institute of Nutrition & Health, Aberdeen, UK

3: Aberdeen Royal Infirmary, Aberdeen, UK

4: University of the Highlands and Islands, Inverness, UK

5: Biomathematics and Statistics Scotland, Rowett Institute of Nutrition & Health, Aberdeen, UK

Scope: Inflammatory status can increase the risk of adverse cardiovascular events linked to platelet activity and involvement of microparticles (MP) released from platelets (PMP), leukocytes (LMP) and monocytes (MMP). These MP carry host cell-derived antigens that may act as markers of metabolic health. Subjects newly diagnosed with type 2 diabetes are offered appropriate standard dietary advice (SDA) but this may not be optimal as inclusion of other nutrients, such as oats, may be more beneficial. The effectiveness of such interventions can be tested by examination of MP activation markers.

Methods and results: Subjects (n=22) with type 2 diabetes participated in a randomised cross-over trial involving 8 wk interventions with either an oat-enriched diet (OAT) or following reinforced SDA. Responses were also compared with pre-intervention habitual (H) intake. OAT reduced the concentrations and proportions of fibrinogen- and tissue factor-related PMP and MMP_{11b}. The main effect of SDA was to reduce fibrinogen-activated PMP. Regardless of chronic intake, a healthy test meal led to post-prandial declines in total PMP as well as tissue factor-, fibrinogen- and P-selectin-positive PMP.

Conclusion: OAT improved risk factors assessed by MP status, even in subjects with type 2 diabetes already well-controlled by diet and life-style alone.

O11

Human serum microRNA profiles after ischaemic stroke

Christopher R Breen¹, Ciaran Groome¹, John D. McClure¹, I. Mhairi Macrae², Andrew H. Baker¹, Jesse Dawson¹, Lorraine M. Work¹

1: Institute of Cardiovascular & Medical Sciences and

2: Institute of Neurosciences and Psychology; College of Medical Veterinary and Life Sciences; University of Glasgow; G12 8TA

Recent pre-clinical^{1,2} & clinical³ studies suggest micro RNAs (miRNAs) may have a role in development of (and recovery after) stroke. Identification of a miRNA signature specific to stroke could serve to facilitate diagnosis and also provide novel therapeutic targets to improve outcomes. We screened serum samples for candidate miRNAs in a cohort of patients with ischaemic stroke and compared them to a cohort of patients with a stroke mimic.

Serum samples were obtained from patients presenting with suspected ischaemic stroke at 48 hours following symptom onset. All patients were assessed by a specialist stroke service and diagnoses were adjudicated in a weekly meeting. A diagnosis of stroke (cases, n=15) was assigned where brain imaging showed an ischaemic lesion in a territory relevant to symptoms. A diagnosis of non-stroke (controls, n=15) was made where brain imaging did not and a firm alternative diagnosis was made. Controls were age and gender matched. Total RNA was extracted and a miRNA array performed using the Openarray platform (758 miRNA represented). Data were analysed using data-assist software & statistical comparisons made between groups where miRNA expression was measured in >70% of at least one sample group.

Of 758 miRNAs, 538 were detected in the serum samples. Comparison of the raw cycle threshold (Ct) values of cases and controls identified 11 miRNAs which were significantly up-regulated in the stroke population (p<0.05): miR-27a, -374, -331, -590-5p, -885-5p, -93, -25, -19b, -24, -451, -21.

miRNAs are present and detectable early after ischaemic stroke. Further, several miRNAs are differentially expressed in cases of stroke compared to age and gender matched controls presenting with mimic. Further study is needed to validate findings in a larger cohort and to identify the pathophysiological significance of individual miRNAs.

1. Dharap A et al. JCBFM. 2009;29:675–87
2. Jeyaseelan K et al. Stroke. 2008;39:959–66
3. Tan KS et al. PLoS One. 2009;4(11):e7689

O12

**MAST CELL DEPENDENT PATHOLOGY MAY BE MEDIATED BY ENDOTHELI-1,
MATRIXMETTALPROTEINASE-9 AND ENDOGLIN, AFTER TRANSIENT MIDDLE
CEREBRAL ARTERY OCCLUSION.**

Craig McKittrick, Catherine Lawrence and Hilary Carswell

*Strathclyde Institute of Pharmacy and Biomedical Sciences, the University of Strathclyde,
161 Cathedral Street, Glasgow, G4 0RE.*

Our previous work showed that genetic mast cell ablation and pharmacological stabilisation significantly reduce oedema, BBB permeability and neutrophil recruitment during the acute phase of reperfusion in experimental stroke.

Activated mast cells release pre-formed tumour necrosis factor-alpha (TNF- α), other cytokines, chemokines, proteases and vasoactive mediators, among others. Therefore, we investigated the expression of an array of proteins in the brain, which may be produced by mast cells directly or induced indirectly in other cell types by the action of mast cells. Additionally, we measured TNF- α concentration. Finally, we measured regional cerebral blood flow to detect any differences in perfusion between the C57BL6 wild type and mast cell deficient C57BL6 Kit^{w-sh/w-sh} mouse strains.

Mice underwent 20 minutes tMCAo, with 5 minutes of reperfusion or 45 minutes tMCAo followed by 45 minutes of reperfusion. Blood flow was monitored throughout using laser Doppler flowmetry. Sham animals underwent the same procedure but did not have the MCA occluded. At termination, ipsilateral hemispheres were analysed by ELISA to determine TNF- α concentration. A proteome profiler array identified the relative expression of 53 proteins related to angiogenesis, within brain homogenates.

At both time points analysed there was no difference in TNF- α concentration in serum and tissue homogenates or in regional blood flow during the occlusion period, between all groups. Also, 20 minutes tMCAo induce similar protein expression profiles in both mouse strains. However, after 45 minutes tMCAo, endothelin-1, matrixmettaloproteinase-9 and endoglin were all expressed in wild type, but were absent in mast cell deficient mice.

Poster Sessions:

P1

Characterisation of signalling mechanisms that underlie P2Y receptor-mediated vasoconstriction of rat intrapulmonary artery

Nawazish-i-Husain Syed¹, Asrin Tengah¹, Charles Kennedy¹ ¹: Strathclyde Institute of Pharmacy and Biomedical Sciences, University of Strathclyde, 161 Cathedral Street, Glasgow G4 0RE, United Kingdom.

P2Y receptors are G protein-coupled receptors that are activated by the endogenous nucleotides UDP and UTP. In arteries, P2Y receptors on arterial smooth muscle cells mediate vasoconstriction (Chootip *et al.*, 2002). We have shown that Ca²⁺ influx via Ca_v1.2 ion channels (Mitchell *et al.*, 2012), Ca²⁺-sensitisation via rho kinase and protein kinase C (PKC) (Tengah & Kennedy, 2007) all contribute to nucleotide-evoked contractions of rat intrapulmonary arteries (IPA). The aim of this study was to determine the relative roles of these signalling components and Ca²⁺-dependent Cl⁻ channels (I_{Cl,Ca}).

5mm rings of IPA were dissected from male Sprague-Dawley rats (200-250g). The endothelium was removed and the rings were mounted under isometric conditions in 1ml baths at 37°C and a resting tension of 0.5g. Tension was recorded by Grass FT03 transducers connected to a Powerlab/4e system. Data were analysed using Student's paired t test or 1-way ANOVA as appropriate.

UDP and UTP (300µM) evoked contractions that reached a peak within 2-3 min. The I_{Cl,Ca} blocker, niflumic acid (1µM) had no effect on contractions to KCl (40mM, n=5), showing that this concentration does not block Ca_v1.2 ion channels or interact directly with the myofilaments to depress smooth muscle contractility. The peak amplitude of responses to UDP (P<0.05, n=5) and UTP (P<0.01, n=5) was, however, reduced significantly by approximately 40-55%. Nifedipine (1µM) also significantly inhibits the peak response to UDP and UTP by about 40-55% (Mitchell *et al.*, 2007) and coadministration of niflumic acid (1µM) plus nifedipine (1µM) for 15 min inhibited contractions to UDP and UTP to the same extent as either agent alone (n=4 each). The rho kinase inhibitor Y27632 (10µM) reduced significantly the peak responses to UDP (P<0.01, n=6) and UTP (P<0.01, n=5) by around 20-30%, whilst the PKC inhibitor, GF109203X (10µM) depressed the response to UDP by about 50% (P<0.01, n=6) and that of UTP by about 20% (P<0.01, n=5). Coapplication of both inhibitors produced significantly greater inhibition than either alone (UDP: P<0.001, n=6; UTP: P<0.01, n=7). Additional co-application of nifedipine (1µM) with Y27632 and GF109203X (10µM) caused no more inhibition of contractions to UDP (n=5), but further depressed the response to UTP (P<0.05, n=5).

These results indicate that I_{Cl,Ca} induces Ca²⁺ influx via Ca_v1.2 ion channels, which mediates about half of the peak contraction amplitude of rat IPA evoked by UDP and UTP. The remainder of the response is due to Ca²⁺-sensitisation via rho kinase and to PKC acting at an as yet unidentified site.

Chootip K *et al.*, (2002). *Br J Pharmacol.*, **137**, 637-646. Mitchell C *et al.*, (2012). *Br. J. Pharmacol.*, **166**, 1503-1512. Tengah A & Kennedy C (2007). *Life Sciences* 2007, **PC366**.

P2

B-vitamin deficiency, gene expression and DNA methylation in vascular smooth muscle cells

Douglas Baird, Linda Petrie, Lynn Pirie, Susan Duthie and Andreas Kolb

Metabolic Health Group, Obesity & Metabolic Health Theme, Rowett Institute of Nutrition & Health, University of Aberdeen, UK

B-vitamin deficiency, especially folate deficiency, is a confounding factor in cardiovascular disease. In mouse models withdrawal of B-vitamins increases the number of atherosclerotic plaques [1]. Folate is critically involved in the one carbon group metabolism of cells. Altered cellular methyl group metabolism may affect (among other things) DNA methylation. Vascular smooth muscle cells derived from atherosclerotic plaques indeed display a decrease in global DNA methylation in comparison to smooth muscle cells derived from healthy vascular tissue [2].

We have analysed how folate deficiency affects gene expression in the rat vascular smooth muscle cell line A7r5 by micro-array and RT-PCR. The genes affected by folate supply were assessed for changes in DNA methylation.

1. Hofmann *et al.*, *J. Clin. Invest.* **107**, 675 (2001).
2. Hiltunen *et al.*, *Vasc Med* **7**, 5 (2002).

P3

Anti-hypertensive Effects of the Aqueous and Its Residual Methanolic Extracts of *Syzygium polyanthum* Wight. Walp. Var. *Polyanthum* Leaves

Wan Amir Nizam Wan Ahmad¹, Azlini Ismail¹

1: School of Health Sciences, Universiti Sains Malaysia

The concoction from the leaves of *Syzygium polyanthum* Wight (walp.) var. *Polyanthum* was traditionally consumed as a treatment of hypertension by Malays. Our previous has showed the ability of aqueous (AESP) and its residual methanolic extracts (met-AESP) in reducing the blood study in normotensive WKY rats. The current study is to further clarify the ability of the extracts to reduce the blood pressure of hypertensive rats and to elucidate its time-course actions. The vehicle (as negative control) and the extracts (AESP and met-AESP at doses of 10, 20, 30, 40, 70, 100 mg/kg) were intravenously administered into male anaesthetized spontaneously hypertensive rats (SHR) to observe for changes in the mean arterial blood pressure (MAP) and the heart rate (HR) responses within 20 min. AESP (20 to 100 mg/kg) and met-AESP (40 to 100 mg/kg) induced significant dose-dependent hypotension (maximum percent changes of MAP by -15.1 ± 2.2 ($p < 0.05$), -19.1 ± 2.8 ($p < 0.01$), -32.2 ± 3.1 ($p < 0.001$), -30.6 ± 4.7 ($p < 0.001$) and 31.3 ± 4.9 ($p < 0.001$)) and (maximum percent changes of MAP by -38.6 ± 7.3 ($p < 0.001$), -47.7 ± 3.2 ($p < 0.001$) and -37.6 ± 1.9 ($p < 0.001$)) respectively, as compared to their respective vehicles. However, only 100 mg/kg AESP caused significant bradycardia (maximum percent changes of HR by -10.9 ± 2.2 ($p < 0.01$)). Dose response curve for AESP and met-AESP-induced hypotension started to be plateau at a similar dose of 40 mg/kg but were significantly different at the dose of 70 mg/kg ($p < 0.05$). The calculated ED₅₀ value for the blood pressure-lowering effects by AESP (26.57 ± 1.2 mg/kg) was lower than met-AESP (33.37 ± 1.0 mg/kg). AESP-induced hypotension (20 to 100 mg/kg) reached its maximum within 0.5 min, as compared to 1.5 min for met-AESP (40, 70 and 100 mg/kg). AESP-induced bradycardia (100 mg/kg) was maximum within 0.5 min and achieved full recovery within 5 min. In conclusion, AESP produced faster and more potent depressor effect on the blood pressure and mild bradycardia at high dose, but its effect was less-sustainable as compared to met-AESP.

P4

Adherence to Heart Failure Therapy and Outcome: A Population Based Study

JL Yeong¹, SA Ogston¹, A Bell², C Hall², D Heather², DH Elder³, AM Choy³, AD Struthers³, CC Lang³

1: University of Dundee, UK

2: Health Informatics Centre, University of Dundee, UK

3: Division of Diabetes and Cardiovascular Medicine, Ninewells Hospital and Medical School, Dundee, UK

Background

Improvements in medical therapy for chronic heart failure (CHF) have resulted in an increase in the number of drugs which patients have to take. As CHF patients are often elderly with multiple comorbid conditions, the resulting polypharmacy could potentially lead to non-adherence to medications. The aim of this study was to determine the prevalence of non-adherence among CHF patients and to determine if non-adherence is associated with a poor outcome.

Methods

We conducted a 10 year retrospective longitudinal cohort study of CHF patients from Tayside in Scotland (population of 450,000) that were started on the angiotensin-converting enzyme (ACE) inhibitor, ramipril, after their incident CHF hospitalisation utilising our established record linkage database linking dispensed prescriptions to other datasets covering socioeconomic status, age, gender, hospital admissions and mortality data. To be included, patients with incident CHF hospitalisation had to have survived their index hospitalisation and completed a month of medication and have not switched to an angiotensin receptor blocker. Adherence was calculated as Proportion of Days Covered, with <80% deemed as non-adherence. Cross-tabulation was utilised to assess the factors associated with non-adherence and its effect on the number of repeated hospitalisation. All-cause mortality was analysed with Cox Regression models.

Results

702 eligible patients (mean age, 75.5±11.3 years) entered into the analysis. 35.9% (mean age, 78.1±11.3 years, 58.7% male) of the cohort were non-adherent and 64.1% (mean age, 74.1±11.1 years, 66.7% male) were considered adherent. Factors associated with non-adherence were male gender, old age (>81 years old), presence of ischaemic heart disease (IHD), chronic pulmonary obstructive disease (COPD) and chronic kidney disease (CKD). Non-adherence was associated with increased number of repeated hospitalisation (p=0.042) and was an independent predictor of all-cause mortality (risk ratio 1.58, 95% confidence interval 1.29-1.95, p<0.001).

Conclusion

Non-adherence to ACE inhibitor therapy was highly prevalent among CHF patients. Male patients, advanced age, presence of IHD, COPD and CKD are associated with non-adherence. Non-adherence was associated with an increase in the number of repeated hospitalisation and predictor of all-cause mortality.

P5

POST-MYOCARDIAL INFARCTION EXERCISE TRAINING REVERSES CARDIAC EXCITATION-CONTRACTION COUPLING ABNORMALITIES BY ACTIVATING CYTOPLASMIC CaMKII

Johnston AS¹, Dunne M¹, Giles WR², Smith GL¹, Kemi OJ¹

1: *University of Glasgow*

2: *University of Calgary*

Abstract: Post-myocardial infarction (MI) heart failure (HF) leads to abnormal excitation-contraction-coupling (ECC) causing cardiac dysfunctions attributable to hyper-activation of CaMKII. In contrast, exercise improves ECC in post-MI HF, but whether this is through CaMKII remains unknown. Our purpose was to test whether exercise reverses ECC dysfunction in post-MI HF through modulation of CaMKII. Permanent coronary artery ligation leading to HF was induced in Wistar rats. Four weeks after, regular treadmill running started (MI-TRN, n=14). Sham-operated (SHAM, n=12) and sedentary MI-HF (MI-SED, n=16) served as controls. MI-HF reduced exercise capacity 16% ($p<0.01$); exercise normalised this. Contractile function of twitch-stimulated cardiomyocytes was assessed using edge-detection and Fura-2 fluorescence microscopy with and without the CaMK inhibitor AIP (5 μ M). MI reduced contraction 40% ($p<0.01$) and increased contraction-relaxation times. This was explained by reduced Ca²⁺ transient amplitude and increased Ca²⁺ rise-decay times. Exercise corrected contraction and contraction-relaxation times, and improved Ca²⁺ handling. AIP abolished the exercise-induced improvement in contraction and Ca²⁺ transient amplitude (both $p<0.01$) and impaired relaxation and Ca²⁺ transient decay times ($p<0.01$) more in MI-TRN than MI-SED. Spontaneous Ca²⁺ waves and sparks were linescan confocal imaged in Fluo-3-loaded cardiomyocytes at normal (1.8mM) and high (5mM) extracellular Ca²⁺. MI increased wave frequency 65% and amplitude 21% ($p<0.01$); this was more pronounced at high Ca²⁺ and reversed by exercise. MI and AIP had no effect on sparks but they were elevated by exercise ($p<0.01$). AIP had no effect on Ca²⁺ wave frequency in MI-SED but increased frequency and amplitude in MI-TRN ($p<0.05$). In conclusion, CaMKII modulated exercise-induced improvements in cardiomyocyte function following MI-HF. In particular, exercise improved sarcoplasmic reticulum (SR) Ca²⁺-uptake and SR-loading by activating CaMKII, whereas Ca²⁺ release parameters were less affected. This suggests that exercise activated cytoplasmic, but not dyadic CaMKII.

P6

The Role of MicroRNA 21 in Porcine and Murine Models of In-Stent Restenosis

Halliday CA^{1*}, Robertson K^{1*}, McDonald RA¹, Kennedy S¹, Oldroyd KG², Douglas G³, Channon KM³, Baker AH¹

1: Institute of Cardiovascular and Medical Sciences, University of Glasgow, UK.

2: Department of Cardiology, Golden Jubilee National Hospital, Clydebank, UK.

3: Department of Cardiovascular Medicine, University of Oxford, John Radcliffe Hospital, Oxford, UK. *Contributed equally

Background: Atherosclerosis within coronary arteries gives rise to luminal narrowing, restriction of blood flow and the development of angina. Percutaneous Coronary Intervention (PCI) with stents is a mainstay of treatment. In-Stent Restenosis (ISR) or luminal renarrowing following PCI is due to the proliferation and migration of smooth muscle cells (VSMCs) and deposition of extracellular matrix (ECM). MicroRNAs (miRs) are small non-coding 19-25 nucleotide RNA molecules that post-transcriptionally regulate gene expression in health but have also been implicated in disease. MiR-21, found in endothelial cells, VSMCs and myofibroblasts is dysregulated in atherosclerotic lesions, following vascular injury and has been implicated in VSMC proliferation and migration (Raitoharju *et al* Atherosclerosis, 2011;219: 211-7, Wang *et al* ATVB, 2011;31:2044-53). We therefore hypothesised that miR-21 promotes cell proliferation and migration leading to ISR.

Methods: Male Welsh Landrace swine 18-22kg received bare-metal (BMS) or drug-eluting (zotarolimus) stents (DES) and were euthanised at 0, 7 or 28 days and 28 days. Total RNA was extracted from one half of the stented porcine coronary arteries. MiR-21 expression levels were measured by quantitative real-time polymerase chain reaction. *In situ* hybridisation was conducted on the other half of the stented vessel. For mouse studies C57/BL6 mice, miR-21 KO and WT controls were used. The aorta of a donor mouse was stented and interposition grafted into a recipient mouse of identical genotype. Grafts were harvested at 0 or 28 days. Following electrochemical dissolution of the stent, tissues were paraffin embedded and morphometric analysis conducted on serial sections taken at regular intervals throughout the stented segment.

Results: In the porcine model (n=4 per group) miR-21 levels were upregulated in the BMS group at both 7 and 28 days by a factor of 5.3±1.1 and 3.8±1.3 respectively (p<0.001 for both) and were also upregulated in the DES group at 28 days by a factor of 5.5±1.6 (p<0.001). The elevated expression of miR-21 was observed within the neointima.

In C57/BL6 mice at 28 days (n=5) vs 0 days (n=8) there was a reduction in luminal area (0.26±0.02mm² vs 0.38±0.02mm², p=0.003). This was due to an increase in neointimal area (0.17±0.04mm² vs 0mm², p=0.0006) with no change observed in either total vessel or medial area. Comparing miR-21 WT and KO mice (n=5 for both groups) at 28 days, no significant difference was observed in neointimal area (0.15±0.02mm² vs 0.12±0.03mm², p=0.41) or neointimal:medial ratio (1.60±0.06 vs 1.43±0.29, p=0.59) and there was no difference in total vessel area or medial area.

Conclusions: Mir-21 is upregulated in porcine coronary arteries following stenting with both BMS and DES. Further work is needed to define the role, if any of miR-21 in the development of ISR in this mouse model and to ascertain utility in the clinical setting.

P7

Quantitative 3-Dimensional Imaging Of Aortic Calcification By Micro Computed Tomography

Carmen Huesa¹, Jose Luis Millan², Rob van 't Hof³ and Vicky E MacRae¹,

1: The Roslin Institute, University of Edinburgh, Easter Bush, Midlothian, United Kingdom, EH25 9RZ

2: Sanford Children's Health Research Center, Sanford-Burnham Medical Research Institute, La Jolla, California.

3: Institute of Genetics and Molecular Medicine, University of Edinburgh, Edinburgh, Lothian, United Kingdom, EH4 2XU

INSTRUCTIONS:

Vascular calcification is a marker of increased cardiovascular risk in Chronic Kidney Disease. Furthering our understanding of the mechanisms that underpin vascular calcification has been advanced considerably by exploiting murine models of aortic calcification. However, the small-scale vascular structures in mice require labor-intensive 2D histomorphometric techniques to visualise regions of calcium deposition, with the extent of calcification often not fully identified. We present here 3D reconstructions of aortae derived from the well-established *Enpp1*^{-/-} mouse model of medial aortic calcification, acquired by micro computed tomography (μ CT). A dual-contrast method for specimen preparation was undertaken, that combined formalin fixation and immersion in fixative with a macro-molecular iopamidol-based contrast agent (Niopam300). To allow tissue differentiation, aortic lumina were filled with corn oil and the aortae submersed in oil for the duration of the scan. Tissues were imaged using a Skyscan 1172 X-Ray Microtomograph. Sequential high-resolution scans in a rotation of 0.3° and an isotropic voxel size of 10 μ m were acquired, reconstructed using NRecon software, analysed and quantified using CTAn software. The selection of specific threshold values in the imaging gray scale detected differences in tissue density, which enabled the identification of areas of calcification. Volumetric reconstructions of calcified and non-calcified aorta were also produced and highly accurate quantification of standardised regions of calcium deposition (400 slices from the subclavian artery) undertaken. Following scanning, aortae were sectioned and stained with Alizarin Red to assess calcium deposition. An excellent correlation between images obtained from μ CT and those obtained by histology was observed. This 3D imaging system provides a powerful tool with which to study aortic calcification progression and potential therapeutic strategies for clinical intervention.

P8

Identification of microRNA target sites in $K_{ir}2.1$ 3' UTR by a novel dual-fluorescent assay

Janet Yarham¹, Anthony Collins¹, Mary McGahon¹, David Simpson¹

1: Centre for Vision and Vascular Science, Queen's University Belfast

MicroRNAs are increasingly recognised as important down-regulators of gene expression. Luciferase-based assays are commonly used for identifying microRNA targets but these have limitations. We report microRNA target identification using a novel functional microRNA targeting assay. The 3' UTR of the inward rectifier K^+ channel $K_{ir}2.1$ was inserted downstream of the mCherry red fluorescent protein sequence in an expression plasmid. MicroRNA, siRNA or non-targeting control (SCR) sequences were inserted into the pSM30 expression vector. Enhanced green fluorescent protein expression was used as an indicator of miRNA expression. HEK293 cells were co-transfected with the pSM30- and mCherry-based plasmids, using the principle that functional targeting of the 3' UTR by the microRNA decreases the cell red/green fluorescence intensity ratio. It was validated with either a siRNA targeting the 3' UTR or miR-1, a previously validated miRNA, and used to investigate targeting of the $K_{ir}2.1$ 3' UTR by miR-212, miR-15b, miR-125b, miR-132 and miR-424 as predicted by bioinformatics. miR-212 was additionally validated by mutation of the putative binding site of the miRNA on the 3' UTR.

Each of these miRNAs is upregulated in heart failure (in particular miR-212 which is upregulated 8 fold), which features downregulation of $K_{ir}2.1$ activity in its pathophysiology. Red/green ratio was significantly lower in miR-1-expressing/miR-212-expressing cells vs. non-targeting controls ($p < 0.001$ miR-1vsSCR and miR-212vsSCR). The effect was attenuated ($p < 0.05$) by mutating the predicted target site. Red/green ratio was also significantly lower in miR-15b, miR-132, miR-424 and siRNA expressing cells vs. non-targeting controls ($p < 0.001$ for all miRNAs and siRNA). Interestingly miR-125b transfected cells had a significantly higher red/green ratio vs. non-targeting controls ($p < 0.001$). This assay allows for a large sample size, increasing the sensitivity and statistical power of the assay, and provides amenability to time course studies as well as adaptability to high-throughput screening. It is potentially therefore a useful tool in the study of miRNAs.

P9

Development of a rabbit model of arteriovenous fistula remodelling

MacAskill, M.¹, Wadsworth, R.M. ¹, Kingsmore, D.², Coats, P.¹

1: Strathclyde Institute of Pharmacy & Biomedical Sciences, University of Strathclyde, Glasgow.

2: Renal Unit, Western Infirmary, Glasgow.

An arteriovenous fistula (AVF) is a vein graft which is created to permit access to the bloodstream allowing haemodialysis to be performed in renal failure patients. These grafts can have significant failure rates, as high 50% at 6 months. Failure is largely due to vascular smooth muscle cell (VSMC) hyper-proliferation, leading to the development of neointima causing stenosis and impaired blood flow. The aim of this study was to develop a rabbit model of AVF remodelling, building on data obtained within the lab from human samples, and identify therapeutics which could be delivered locally to reduce remodelling.

The proposed model was an AVF created between the femoral artery and vein of a New Zealand white rabbit. Over an initial period of 28 days, maturation of the vein was evident by an increase in blood velocity and medial/adventitial remodelling. A subsequent 28 day period allowed cannulation injury, analogous to the haemodialysis procedure, to be performed with and without the addition of topical diclofenac. All veins underwent remodelling measured by an increase in vein wall thickness, with the injury group showing the biggest increase. With diclofenac treatment in injured vessels, vein wall thickness decreased to a level similar to animals which received no injury.

P10

Selective smooth muscle cell ETB receptor deletion abolishes sarafotoxin 6c-mediated vasoconstriction

Patrick WF Hadoke, Karolina M Duthie, Eileen Miller, Elise van der Putte, Sibylle Christen, Yuri V Kotelevtsev and David J Webb.

BHF/ University Centre for Cardiovascular Science, University of Edinburgh, Scotland, UK.

Endothelin-1 (ET-1)-dependent vasoconstriction is predominantly mediated by the ETA receptor in smooth muscle cells. ETB receptors, which are expressed in both the smooth muscle and endothelial cells, can also mediate contraction of some vessels. We sought to clarify the role of ETB receptors in vasoconstriction by generating mice with selective smooth muscle cell deletion of these receptors.

Methods: Mice with smooth muscle selective deletion of the ETB receptor were generated using cre-lox combination and confirmed by genotyping. Sections of trachea, mesenteric artery and mesenteric vein were isolated from adult, male control (C57Bl6), smooth muscle cell-selective ETB knockout (ETB sm22Cre) and wild type (FF^{-/-}) mice. These were suspended in myography chambers (containing physiological salt solution; 37°C) to allow construction of concentration-response curves to phenylephrine (PhE; 10⁻⁹-3x10⁻⁵M), ET-1 (10⁻¹¹-3x10⁻⁷M), sarafotoxin 6c (S6c; 10⁻¹¹-3x10⁻⁷M), and acetylcholine (ACh; 10⁻⁹-3x10⁻⁵M). Some sections were exposed to ETA or ETB receptor antagonists. In some cases arteries were incubated in culture medium (DMEM; 24 hours; 37°C) before functional analysis.

Results: S6c produced concentration-dependent contractions in freshly-isolated trachea and mesenteric veins. Freshly-isolated mesenteric arteries did not contract in response to S6c but responses were induced by incubation in culture medium. In all tissues, S6c-mediated contraction was abolished by the ETB antagonist (A192621, 100nM).

Selective genetic deletion of ETB from smooth muscle cells reduced, but did not abolish, S6c-mediated contraction in the trachea. In femoral arteries from these mice acetylcholine-mediated relaxation and contractile responses to PhE, ET-1 and potassium were unaltered. S6c-mediated contraction, however, was abolished both in the mesenteric artery and in the mesenteric vein.

These results demonstrate successful use of cre-lox methodology to generate mice with selective deletion of ETB receptors from the vascular smooth muscle. These mice will provide a useful resource for investigating the physiological (blood pressure regulation, vasoconstriction) and pathophysiological (neointimal lesion formation; angiogenesis) roles of the ETB receptor in vascular smooth muscle.

P11

Spontaneous Ca²⁺ transients in rat pulmonary vein cardiomyocytes following electrical field stimulation

Alasdair Henry¹, Professor Andrew Rankin², Dr Edward Rowan¹, Dr Robert Drummond¹

1: Strathclyde Institute of Pharmacy and Biomedical Sciences, University of Strathclyde.

2: College of Medical, Veterinary and Life Sciences, University of Glasgow.

Atrial fibrillation (AF) is a significant cause of morbidity and mortality and occurs when the electrical activity of the atria is no longer under the control of the sino-atrial node. In most cases of AF, the source of electrical activity is the pulmonary vein (PV). The PV has an external sleeve of cardiomyocytes and it is these cells that are believed to be responsible for its arrhythmogenic propensity. The mechanisms underlying the ectopic activity in the PV are unclear; but it is thought that intracellular Ca²⁺ may play an important role.

We have previously observed spontaneous Ca²⁺ transients in cardiomyocytes of the rat PV, which are due to the release of Ca²⁺ from the sarcoplasmic reticulum (SR). We believe that these spontaneous Ca²⁺ transients are unable to trigger action potentials in the PV cardiomyocytes, because of their asynchronous nature. However, should spontaneous Ca²⁺ transients become more synchronous, then they would be capable of affecting the electrical activity of the PV. Thus, the aim of this study was to determine what effect a period of electrical stimulation, together with various pharmacological interventions would synchronise the spontaneous Ca²⁺ transients of PV cardiomyocytes.

Male Sprague-Dawley rats (175-250 g) were euthanised by cervical dislocation and the PV was isolated. The Ca²⁺ sensitive dye, fluo-4 AM (10 μM) was used to monitor intracellular Ca²⁺ in cardiomyocytes within an intact region of the PV.

Under basal conditions, the frequency of spontaneous Ca²⁺ transients was 0.45 ± 0.06 Hz, and this was significantly increased to 0.59 ± 0.05 Hz (P<0.001) following electrical field stimulation (3 Hz for 5 s). This effect was enhanced in the presence of isoprenaline (10 μM), where the frequency of the spontaneous Ca²⁺ transients increase from 0.5 ± 0.07 Hz under basal condition to 0.73 ± 0.04 Hz after electrical stimulation (P<0.001). Increasing the extracellular Ca²⁺ concentration by 2 mM further enhanced this effect, with the frequency of spontaneous Ca²⁺ transients increasing from 0.45 ± 0.05 Hz under basal conditions to 0.91 ± 0.07 Hz after stimulation (P<0.001).

This study has shown that following electrical field stimulation there is an increase in the frequency of the spontaneous Ca²⁺ transients in PV cardiomyocytes. This is most likely due to an increased SR Ca²⁺ load, which can be further enhanced by isoprenaline and raising the extracellular Ca²⁺ level. It should be noted that none of these manipulations resulted in the synchronisation of the spontaneous Ca²⁺ transients.

P12

GPR35 as a novel therapeutic target of cardiovascular disease

Jennifer E. Lappin¹, Stuart A. Nicklin², Graeme Milligan¹

1: Molecular Pharmacology Group, Institute of Molecular, Cell, and Systems Biology, College of Medical, Veterinary, and Life Sciences, University of Glasgow, Glasgow, United Kingdom

2: Institute of Cardiovascular and Medical Sciences, College of Medical, Veterinary, and Life Sciences, University of Glasgow, Glasgow, United Kingdom

GPR35 is a poorly characterised G protein-coupled receptor which is activated endogenously by kynurenic acid and couples to G α 13, a G protein involved in regulation of cellular motility and proliferation. The role of this receptor in CVD is not well described, although recent findings indicate it has a role in blood pressure regulation and cardiomyocyte hypertrophy (Min *et al.*, 2010). Thus, exploring GPR35 function is important and may define it as a therapeutic target for cardiovascular disease, hypertension and related end organ damage. We have shown that GPR35 is highly expressed in the heart and kidney of the spontaneously hypertensive stroke prone rat (SHRSP) and that kidney expression is significantly higher in SHRSP than WKY at the onset of hypertensive end organ damage. We have previously demonstrated that a number of synthetic compounds including zaprinast, pamoic acid and cromolyn are potent ligands at GPR35 and the recent identification of two antagonists, CID-2745687 and ML145, has supported our efforts to further dissect the function of GPR35 in an *in vitro* wound healing assay. Here we demonstrate that upon GPR35 agonist activation, the migratory capacity of human primary saphenous vein smooth muscle cells (HSV SMCs) is enhanced and that this migratory effect is prevented in the presence of GPR35 antagonists and ROCK inhibitors. We plan to investigate this pro-atherosclerotic response in an *ex-vivo* setting, specifically assessing neointima formation in intact tissue from human saphenous veins. We hope that further investigation of GPR35 in this setting will help to dissect its role in CVD and highlight it as a novel therapeutic target.

P13

Comparison of the agonist activities of treprostinil and naxaprostene in systemic blood vessels

Nawazish-i-Husain Syed* and Robert L. Jones

Strathclyde Institute of Pharmacy and Biomedical Sciences, University of Strathclyde,

161 Cathedral Street, Glasgow G4 0RE, United Kingdom.

Treprostinil, a prostacyclin analogue, is used to treat pulmonary hypertension. However, the mechanism of action whereby this drug modifies the pathophysiological status may involve more than prostacyclin (IP) receptors, as Whittle et al (2012) have shown that it activates human recombinant prostanoid DP₁, EP₂ and IP receptors.

In view of the recent emergence of highly selective EP₂ receptor antagonists (e.g. PF-04418948; Forselles et al., 2011), it was decided to determine whether our current armory of prostanoid antagonists was adequate to elucidate the complex pharmacology of treprostinil. Treprostinil lacks the ether oxygen moiety at C6-9 present in prostacyclin (PGI₂) and has a benzene ring inserted in its α -chain. Naxaprostene also has both functionalities and we decided to compare its inhibitory profile with that of treprostinil.

In the current study, we have used isolated preparations of rabbit saphenous vein (rSV) and inferior vena cava (rVC). 5 mm rings were dissected from male rabbits (1.5-2.5 kg) and were mounted under isometric conditions (resting tension of 0.75 – 1.0 g) in 10 ml baths at 37°C. Contractions were elicited by adding histamine and phenylephrine (300-600 nM) respectively. We have used BW-245C, ONO-AE1-259, TCS-2510 and AFP-07 as selective DP₁, EP₂, EP₄ and IP agonists respectively. The corresponding antagonists were BW-A868C and MK-0524, ACA-23 (same series as PF-04418948), GW-627368 and RO-1138452 (Jones et al., 2009).

A simple antagonist reversal protocol showed that both preparations contain inhibitory DP₁, EP₂, EP₄ and IP receptors. In further experiments, preparations were pretreated with 3 of the antagonists (e.g. BW-A868C / ACA-23 / GW-627368), followed by cumulative doses of treprostinil or naxaprostene, followed by the fourth antagonist (CAY-10441) in an attempt to reverse the relaxation. In this way we could apportion DP₁, EP₂ and IP agonism to treprostinil, but only IP agonism to naxaprostene. In some preparations naxaprostene behaved as a partial agonist. The relevance of these findings to the therapeutic use of prostacyclin analogues will be discussed.

References: af Forselles KJ, Root J, Clarke T, Davey D, Aughton K, Dack K and Pullen N. (2011). *Br. J. Pharmacol.*, 164: 1847-1856. Jones RL, Giembyez MA and Woodward DF. (2009). *Br. J. Pharmacol.*, 158: 104-145. Whittle BJ, Silverstein AM, Mottola DM and Clapp LH. (2002). *Biochem. Pharmacol.*, 84: 68-75.

P14

MAPKAP 2/3: A NOVEL TARGET TO SEQUESTER CHOLESTEROL INDUCED CARDIOVASCULAR DISEASES *IN VIVO*?

Naveed Akbar¹, Matthias Gaestel², Jill J. F. Belch¹, Faisal Khan¹

1: Vascular and Inflammatory Diseases Research Unit, University of Dundee, Dundee, UK

2: Institute of Physiological Chemistry, Hannover Medical University, Hannover, Germany

Background and Aims

Atherosclerosis is an inflammatory condition and is regarded as the underlying pathology in many cardiovascular diseases (CVD). However effective therapeutic intervention has been limited in this area. The p38 pathway is responsible for pro-inflammatory gene expression; we examine the downstream targets mitogen-activated protein kinase-activated protein kinases (MAPKAPKs) 2/3 and their role in CVD as potential targets for future therapy.

Methods

Skin microcirculation was assessed on the flanks of 12 week old anaesthetised male C57/B/6 MAPKAPK 2/3 knock-out (KO) ($n=24$) and wild-type (Wt) ($n=24$) mice over a 20 week period. Wt and KO mice were subdivided and either fed normal rodent chow ($n=12$) or a high cholesterol diet (2%) ($n=12$). Laser Doppler imaging (LDI) with iontophoresis of acetylcholine (ACh) and sodium nitroprusside (SNP) were utilised to assess vascular function. Results expressed as skin perfusion in arbitrary units (AU) \pm SEM. Student T-test was used for statistical significance analysis .

($p = <0.05$).

Results

There were no significant differences for baselines values (ACh) between groups (Wt 316 ± 18 AU and KO 290 ± 14 AU). Wt chow fed animals maintained vascular function for ACh (336 ± 15 AU). Cholesterol fed Wt animals show depleted ACh responses (260 ± 12 AU) ($p = 0.007$). MAPKAP 2/3 KO mice maintain vascular function for ACh on chow (297 ± 13 AU) and cholesterol (311 ± 23 AU). There were no significant differences in SNP.

Conclusions

MAPKAPKs 2/3 KO mice are resistant to cholesterol induced vascular dysfunction at the level of the endothelium, unlike Wt cholesterol fed animals. Endothelial dysfunction is a clinical hallmark of atherosclerosis, potential inhibition of MAPKAPKs 2/3 may prove advantageous by preventing vascular lesion formation and/or progression.

P15

Sudden death referrals to the West of Scotland Inherited Cardiac Conditions Clinic: an overview

Catriona Brown¹, Victoria Murday², Denise Oxnard², Joan Anusas³, Edward Tobias⁴ Christian Delles¹, Iain Findlay³

¹*Institute of Cardiovascular and Medical Sciences, University of Glasgow, UK*

²*West of Scotland Regional Genetics Service, Southern General Hospital, Glasgow, UK*

³*Inherited Cardiac Conditions Service, Western Infirmary, Glasgow, UK*

⁴*Duncan Guthrie Institute, University of Glasgow, UK*

OBJECTIVES: The West of Scotland Inherited Cardiac Conditions Clinic (ICC) was established in 2007 to meet best practice guidelines for families with arrhythmias and sudden cardiac death, as outlined in the 2005 National Framework for CHD. This service comprises a cardiologist, clinical geneticist, genetic counsellor and a cardiomyopathy nurse. Funding for molecular genetic analysis is provided by the National Services Division (NSD) of the Scottish Government.

DESIGN AND METHODS: We conducted an audit of sudden death referrals to the ICC clinic up to 31st August 2012. At post-mortem, after toxicology investigations but prior to genetic testing, sudden deaths were categorised as follows: “unascertained”, “sudden adult/arrhythmic death (SADS)”, “sudden infant death” (SIDS), “sudden unexplained death in childhood”, “other” (including structural heart diseases, drugs/alcohol, seizures).

RESULTS: 78 pedigrees had completed evaluation at time of audit. Mean age at time of death was 29±15yrs and 70.5% were male. In 35/78 (44.9%) referrals, the proband had a structurally normal heart. In this group mean age was 25±14yrs and 62.9% were male. These cases had been classified as “unascertained” 10, “SADS” 14, “SIDS” 4 and “other” 7. Molecular testing was possible in 24/35 (68.6%). Long QT syndrome genes (*KCNQ1*, *KCNH2*, *SCN5A*, *KCNE1*, *KCNE2*) were tested in 100% of these cases. In addition ARVC genes (*PKP2*, *DSP*, *DSG2*, *DSC*) were tested in 10/24 (41.7%), CPVT gene (*RYR2*) in 7/24 (29.2%), and a variety of other genes were also tested. Overall two pathogenic mutations (*KCNQ1*, *SCN5A*) and nine variants (2 *KCNQ1*, 2 *SCN5A*, 2 *RYR2*, 2 *PKP2* and 1 *DSG2*) were detected in those with a structurally normal heart. Low/moderate levels of alcohol were found in 10/35 (28.6%) cases, and 3 of the 10 also had a low/moderate level of recreational drugs. In 10/35 (28.6%) families there was a family history of two sudden deaths, including the proband, and 4/35 (11.4%) families experienced three or more sudden deaths. All first degree relatives had been offered an ECG and ECHO as baseline investigations, and ETT, 24hr tape, flecainide/ajmaline tests and cardiac MRI were also offered where appropriate.

CONCLUSIONS: The yield of pathogenic mutations in sudden death cases with structurally normal heart is 2/24 (8.3%), lower than reported in the literature (15-33%). However, the number of sudden death cases referred to the ICC is lower than National statistics would suggest. This audit also highlights the challenges of genetic testing in the discovery of variants which need to be considered carefully and often require further evaluation.

P16

Drug Delivery from Coronary Stents: insights from mathematical models

McCormick C¹, McGinty S², Wadsworth RM³, Kennedy S⁴, Wheel M¹, Oldroyd K⁵, McKee S²

1: Engineering, University of Strathclyde

2: Mathematics and Statistics, University of Strathclyde

3: Strathclyde Institute of Pharmacy and Biomedical Sciences

4: Institute of Cardiovascular and Medical Sciences, University of Glasgow

5: West of Scotland Regional Heart and Lung Centre, Golden Jubilee Hospital

Although drug-eluting stents (DES) are now commonly used in the treatment of coronary heart disease, they remain unsuitable for certain patient groups and lesion types and persistent concerns around delayed vessel healing mean that prolonged anti-platelet therapy is still required. There is thus much research effort dedicated towards the development of improved DES designs. A key factor in any successful DES is the drug release profile. However, current methods of optimising such profiles are time intensive, costly and require large numbers of animals.

We have developed a series of mathematical models of drug release from DES. Our most sophisticated model includes the three regions (polymer, media, and adventitia) and within the media we include smooth muscle cells and atherosclerotic plaque material. We are also able to model the effect of different fluid mass transport mechanisms across the artery wall.

In the present study, we firstly sought to validate our models in a series of in vitro elution studies. Cypher Stents were immersed in a physiological release medium (37°C) for periods up to 60 days, with samples being analysed for rapamycin content using UV-spectroscopy at various time points. We found good agreement between the in vitro release profiles obtained and the model predictions. In our in vivo model validation study, we deployed a total of 12 Yukon stents coated with the anti-oxidant, succinobucol, into the coronary arteries of six Male Large-White/Landrace pigs. Each pig was killed at a different time point between 1 hr and 28 days following stent deployment. Drug remaining on the stent and within the tissue was then quantified using HPLC. We found that our model accurately predicted drug release from the stent although significant variations were found between the model output and predictions of drug level within the artery wall.

The good correlations we have achieved for in vitro and in vivo drug release profiles are based on the relatively well defined problem of mapping drug release using reaction/convection/diffusion equations. However, on release from the stent, the modelling challenge becomes significantly more complex. More sophisticated modelling approaches, incorporating the complex artery geometry and time dependent nature of the input variables, are likely to be required to enhance the utility of mathematical models for drug-eluting stent design.

P17

Distribution and expression pattern of the cardiac slow delayed rectifier channel in the human heart

Craig Docherty^{1, 2, 3}, Edward Rowan¹, Sharron Dolan², David Bunton³

1: University of Strathclyde, Glasgow

2: Glasgow Caledonian University

3: Biopta Ltd, Glasgow

Introduction

The IKs channel is a known cardiovascular liability for drugs that prolong the cardiac action potential, suggesting a role in acquired long QT-like disorders (Towart et al, 2009). Defects in IKs are also the cause of several inherited diseases that can cause disturbances in heart rhythm such as long QT syndrome. *In-vitro* the voltage-gated potassium channel KCNQ1 (Kv7.1) associates with the accessory subunit KCNE1 (minK) to form an outward current with kinetics closely resembling that of the cardiac slow delayed rectifier current (IKs) (Sanguinetti et al, 1996). The aim of this study was to determine the distribution of KCNQ1 and KCNE1 mRNA in healthy human hearts and then assess the distribution of the ion channel in order to determine specific regions that might be at risk of inherited and acquired cardiac arrhythmias.

Methods Real-time PCR was used to characterise KCNQ1 and KCNE1 mRNA expression in several different regions of non-diseased adult human hearts (n=6). Distribution of KCNQ1 and KCNE1 proteins was assessed using immunocytochemistry staining of cryo-sections of human heart muscle. Staining was visualized using confocal microscopy.

Results Real-time analysis revealed that KCNQ1 mRNA is expressed in significantly higher levels than KCNE1 in all 8 cardiac areas investigated (all P < 0.001). Further analysis revealed that KCNQ1 mRNA levels are similar between all areas, whereas KCNE1 mRNA expression was much more variable, however, there was no significant difference detected. Both KCNQ1 and KCNE1 proteins were expressed in cardiac myocytes from various regions in the human heart and show some evidence of co-localization, mainly restricted to the cell membrane.

Conclusions The high level of KCNQ1 mRNA and protein expression relative to KCNE1, suggests that even low levels of KCNE1 may modulate the KCNQ1 current. Evidence of KCNQ1 and KCNE1 co-localization indicates potential interactions on the myocyte membrane contributing to cardiac action potential regulation.

References Sanguinetti. MC, *et al* (1996) Coassembly of K(V)LQT1 and minK (IsK) proteins to form cardiac I(Ks) potassium channel. *Nature* **384**(6604):80-83

Towart. R, *et al* (2009) Blockade of the I(Ks) potassium channel: an overlooked cardiovascular liability in drug safety screening? *J Pharmacol Toxicol Methods* **60**(1):1-10

P18

Identification and functional validation of osteopontin as a candidate gene for left ventricular mass index in the stroke prone – spontaneously hypertensive rat.

W. Crawford¹, A Monkeviciute ¹, S Tsiropoulou ¹, JD McClure ¹,

AF Dominiczak¹, D Graham¹, MW McBride¹

1: Institute of Cardiovascular & Medical Science, University of Glasgow,

G12 8TA

Background. The stroke-prone spontaneously hypertensive rat (SHRSP) is an excellent inbred model of human cardiovascular disease, which develops increased left ventricular mass index (LVMI) in young animals, prior to the onset of hypertension. The aim of the study was to use a combination of chromosome 14 congenic strains (SP.WKYGla14a and WKY.SPGla14a) and gene expression profiling to identify positional candidate genes within the chromosome 14 congenic interval. Furthermore, to use metabolomic profiling to identify key metabolites involved in the cellular process of hypertrophy.

Methods. Cardiac gene expression profiles were determined by Illumina microarray from male, day 1 neonates from SHRSP, WKY, SP.WKYGla14a and WKY.SPGla14a congenic strains (n=4). The expression data was quantile normalized and differential expression was assessed by Rank Product analysis (false discovery rate (FDR) < 0.05). Positional candidate genes mapping to the congenic interval were validated by qRT-PCR (n=4/strain). DNA sequence analysis identified single nucleotide polymorphisms (SNP's) within the promoter and open reading frame (ORF) regions. Transcription factor (TF) binding sites in the promoter region were investigated by Transfac analysis. Osteopontin (*Spp1*) over expression was compared to angiotensin-II treatment in a model of hypertrophy (cardiomyoblast H9c2 cell line) and metabolome profiling was also undertaken.

Results. Filtering the expression profiles across four strain comparisons (FDR< 0.05), identified differential expression of 4 genes – osteopontin (*Spp1*), hydroxysteroid 17 beta dehydrogenase (*Hsd17b13*), zinc finger protein (*Zfp644*), and Ras related associated with diabetes (*Rrad*) and validated by qRT-PCR. *Spp1* sequencing identified 2 SNP's in the promoter region (-2258 and -1644 bp) and 2 SNP's within the ORF (+450 and +559 bp). The promoter SNP's lie within a number of potential TF binding sites: YY1, Twist, GATA 1, GATA 2 and GATA 3. Analysis of the SNP's within the ORF identified a conserved change in amino acid in the SHRSP (Isoleucine to Leucine). Over-expression of *Spp1* cDNA from SHRSP in H9c2 cell line results in a significant increase in cell size compared to controls. Metabolomic profiling of these cells comparing the effects of angiotensin II treatment and *Spp1* over expression implicated different potential mechanisms leading to an increase in cell size, including increased reactive oxygen species and an increase in proinflammatory cytokine signalling.

Conclusion. Using a combination of congenic strains, microarray gene expression analysis and metabolomic profiling identifies osteopontin as a positional and functional candidate gene for left ventricular mass index in the SHRSP.

P19

Distinctive profile of isomiR expression and novel microRNAs in rat heart left ventricle

Aideen Daly, Mary K McGahon, Janet M Yarham, Jasenka Guduric-Fuchs, Lyndsey Ferguson, David A Simpson, Anthony Collins*

Centre for Vision and Vascular Science, Queen's University Belfast, Block A, Institute of Clinical Sciences, Grosvenor Road, Belfast BT12 6BA

**Corresponding author*

Email address: anthony.collins@qub.ac.uk

The role of microRNAs (miRNAs) in post transcriptional gene expression is becoming increasingly topical as a potential therapy for a number of heart conditions including arrhythmias, cardiomyopathies and heart failure. Advances in Next Generation Sequencing (NGS) Technologies have allowed for more sensitive identification of known and novel miRNA profiles in the heart than previously achievable. The distribution of ion channels, contractile proteins and gap junctions are known to vary across the wall of the ventricle and is thought to underlie the vital differences in action potential shape and duration as well as contractile function; however, little is known about the distribution of miRNA across the ventricle. To address this, miRNA expression across the left ventricular wall was profiled using NGS on tissues extracted from 3 male 8 month old Sprague Dawley rat hearts. NGS of mid-myocardium revealed 154 previously identified rat annotated miRNAs and 68 novel orthologs at ≥ 10 raw reads, with 48 of the rat annotated miRNAs and 3 novel miRNAs detected at a significant level (≥ 1000 RPMM of total annotated). Analysis of the isomiR sequences associated with each annotation indicated that the mature sequence as published in miRBase (v18) was not always the highest detected sequence.

Target prediction of the 10 highest detected miRNAs revealed potential targeting of Ubiquitin Mediated Proteolysis, MAPK signalling and Wnt signalling pathways which have all been implicated in remodelling events in the heart. Indeed, miR-486 which was our second highest detected miRNA is highly implicated in remodelling via PI3K/AKT signalling (Small et al, 2010). This miRNA is unique in our top ten as it is the only miRNA whose sequence has not yet been reported in miRBase for its presence in the rat genome. Here we report the first cloning and sequencing of this gene in rat.

miR-486 was also detected at different levels endo->epi-cardium using NGS (1.37 +/- 0.35 n=3) which was confirmed by qPCR (expression endo->epi-cardium by a mean factor of 1.336; S.E. range 1.298 - 1.401; $p < .01$; n = 4). miR-486 is predicted to target NCX1 (TargetScan 6.2), a protein which displays epi->endo-cardial differential expression; additionally miR-21 (endo->epi-cardium) is predicted to target Calcineurin A α which not only is expressed epi->endo-cardium but is known to upregulate SERCA2 and NCX1. Therefore miR-486 and miR-21 may potentially influence transmural differences in intracellular Ca²⁺ handling.

There is mounting evidence to suggest a physiologically important role for miRNA isoforms (isomiRs) in the regulation of gene expression in cardiac pathologies. As a result, the potential for miRNA based therapies in the treatment of a wide range of heart conditions is increasing.

P20

A COMBINED APPROACH ON INTEGRATED FUNCTIONAL GENOMICS DATA TO PRIORITIZE CANDIDATE GENES IN THE STROKE-PRONE SPONTANEOUSLY HYPERTENSIVE AND WISTAR KYOTO RATS.

Mohammed Dashti¹, Klio Maritou², Santosh Atanur², Tim J. Aitman², Anna F. Dominiczak¹, Delyth Graham¹, Rainer Breitling³, John D. McClure¹, Martin W. McBride¹

¹Institute of Cardiovascular & Medical Science, University of Glasgow, Glasgow, UK; ²MRC Clinical Science Centre, Faculty of Medicine, Imperial College, London, W12 0NN, UK; ³Computation & Evolutionary Biology, University of Manchester, Manchester, UK.

Introduction: The stroke-prone spontaneously hypertensive rat (SHRSP_{Gla}) is an excellent model for human cardiovascular disease. Quantitative trait locus (QTL) were identified on chromosome 2 for systolic blood pressure and were validated by the construction of congenic strain. This study aims to identify positional candidate genes which contribute to the SHRSP_{Gla} phenotype by analysing SHRSP_{Gla} and WKY_{Gla} genome sequence, and gene expression data.

Method: Illumina paired-end reads from the SHRSP_{Gla} and WKY_{Gla} were mapped to reference genome of Brown Norway (BN) using Burrows Wheeler Aligner. Genome Analysis Toolkit was used to discover variants call between the SHRSP_{Gla} and WKY_{Gla}. Ensembl Variant Effect Predictor tool was used to annotate the sequence variants. Ingenuity pathway analysis (IPA) was used to provide insights into the impact of SHRSP_{Gla} and WKY_{Gla} genomic variants. Significantly differentially expressed positional candidate genes identified by Partek® Genomics Suite (ANOVA) in kidney tissue which harbour protein coding sequence variants were prioritised. Further candidate genes were identified by clustering analyses of set of genes that correlated with SHRSP_{Gla} validated genes using Biolayout Express3D.

Results: More than 90% of reads were mapped to reference genome of SHRSP_{Gla} at 20x and WKY_{Gla} at 26x coverage. Genomic difference distribution of 1,163,332 single nucleotide polymorphisms (SNP) and 213,130 insertions and deletions of DNA segments (INDEL) between SHRSP_{Gla} and WKY_{Gla} were not uniform. IPA biological interpretation of SHRSP_{Gla} and WKY_{Gla} genomic variants implicate networks, diseases and pathways that regulate cardiovascular disease. Significantly differentially expressed genes in kidney that associated with 769 non-synonymous coding, 5 stop gained, 24 frame shift coding SNPs and INDELS within the congenic regions prioritised a number of candidate genes. One of the identified candidate genes, *Gstm1*, was previously validated as positional and functional candidate for hypertension in SHRSP_{Gla}. Six genes were identified in a cluster that correlated with *Gstm1* in which *Gstm7*, *Ampd2*, *Atp11b*, *Pik3r1* mapped to chromosome 2 congenic intervals.

Conclusion: We have shown that the integration of sequence variants and gene expression data between SHRSP_{Gla} and WKY_{Gla} has implicated positional and/or functional candidate genes which can contribute to SHRSP_{Gla} blood pressure regulation.

P21

Myocardial Fat in Cardiovascular Disease; A Diabetic Perspective

Deirdre Cassidy¹, SJ Gandy^{2,3}, SL Duce¹, S Matthew¹, P Martin², F Khan¹, RS Nicholas^{2,3}, JG Houston^{1,2}

1: The Institute of Cardiovascular Research (TICR), University of Dundee, Ninewells Hospital, Dundee.

2: Clinical Radiology, 3: Medical Physics, NHS Tayside Academic Health Sciences Centre, Ninewells Hospital, Dundee.

Lipid accumulation in cardiac myocytes is an early manifestation in the pathogenesis of Type-2 Diabetes Mellitus. MRI has become gold standard in cardiac functional and structural assessments but other quantitative fat assessments may provide additional prognostic information. Myocardial fat can be subdivided into epicardial adipose tissue (EAT), enclosed by the visceral pericardial sac, and paracardial layer, anterior to EAT. It has been postulated that the outer paracardial layer remains relatively inert however EAT hosts a metabolic active role. This study aims to examine the physiological or pathological role of EAT in a blinded diabetes population with and without cardiovascular (CV) disease and correlate these measure with left ventricular (LV) assessment.

On a standard 4-chamber cardiac MR image, acquired on a 3T Siemens Trio (Erlangen, Germany), manual contours were placed dividing the two fat layers for each patient (n=20) and reviewed by an experienced radiologist. These measurements were then correlated with standard LV assessment.

EAT was found to be associated with lower ejection fraction, increased left ventricular mass and abnormal diastolic function.

Recent studies are beginning to highlight epicardial fat playing an active role as a cardiometabolic risk factor. Pericardial fat has shown to be less associated with prediabetic heart morphology or serving as a therapeutic target and more with the modulation of coronary arteries. Further work will include the unblinding of the study and examination of fat volumes with LV function and its interaction with traditional CV risk factors.

P22

Expression and localisation of H₂S metabolising enzymes in the murine myocardium and liver

Barry Emerson¹, Ian Dransfield², Nik M Morton¹, Gillian A Gray¹

1: *British Heart Foundation Centre for Cardiovascular Science, QMRI, University of Edinburgh*

2: *Medical Research Council Centre of Inflammatory Research, QMRI, University of Edinburgh*

Background New interventions are required to prevent the loss of cardiomyocytes associated with myocardial ischemia and with the reperfusion injury that follows revascularisation. Recent studies have shown that compounds releasing hydrogen sulfide (H₂S) can have cardioprotective effects¹. However, these compounds are generally effective only at high (μM) concentrations and release is not well controlled, increasing the potential for cytotoxicity. H₂S is produced endogenously and targeting the pathways that regulate availability in heart may be a more promising therapeutic approach. The present study aimed to characterise the distribution of the H₂S synthesising enzymes, cystathionine beta-synthase (CBS), cystathionine gamma-lyase (CSE) and mercaptopyruvate sulfurtransferase (MPST), and of H₂S degrading enzyme, thiosulfate sulfurtransferase (TST) in the murine heart and in liver, an important site of H₂S metabolism.

Methods RNA and protein were prepared from heart and liver collected from 10wk old male C57BL/6J mice for quantitative RT-PCR and Western blotting. Further tissue was formalin fixed, processed and wax embedded before sectioning for immunohistochemistry.

Results qRT-PCR showed high relative gene expression for all H₂S metabolising enzymes in the liver. Cardiac tissue displayed high relative gene expression of TST, MPST & CSE and low expression of CBS. Western blots confirmed the presence of protein for TST & all H₂S synthesising enzymes within heart & liver homogenates. Immunohistochemical staining of fixed tissue sections located CSE to vascular smooth muscle in the heart, while CBS & MPST were found in the vascular endothelium. Cardiomyocytes were immunoreactive for all enzymes. In hepatocytes, immunoreactive TST, CBS & MPST are found in hepatocytes throughout the liver, while CSE immunoreactivity is notably intensified around the central vein, responsible for hepatic venous return.

Conclusion The murine myocardium and liver have the capacity to regulate local H₂S availability via three separate synthetic pathways at least one degradative pathway which have distinctive cellular localisations. Future studies will investigate whether metabolic & synthetic enzyme expression and H₂S availability is differentially regulated following ischaemia and reperfusion.

1. Elsey, D.J., *et al.* (2010) *Cell Biochem Function*, 28,95-106.

BE is funded by a British Heart Foundation PhD studentship (FS/10/49/28675).

P23

Evaluation of laboratory tests for aspirin response in patients with stable cardiovascular disease

Isobel Ford¹, Samia Nacef^{1,2}, Fahad Aldhafeeri^{1,2}, Louise Mitchell¹, Julie Brittenden¹

1: Division of Applied Medicine, School of Medicine & Dentistry, University of Aberdeen

2: MSc Clinical Pharmacology course 2011-12, College of Life Sciences and Medicine, University of Aberdeen

Aims Response variability can reduce the effectiveness of antiplatelet drugs in secondary prevention. However, laboratory monitoring remains rarely used outside of research. Not all of the tests available are direct measures of antiplatelet drug effects, and some may be influenced by factors other than platelet inhibition. We aimed to compare the usefulness of a range of platelet aggregation and activation assays for aspirin responsiveness, and to determine the influence of adhesive proteins, fibrinogen and von Willebrand factor (vWF).

Methods Blood samples were obtained from 50 aspirin-treated (75mg daily) adults with stable coronary artery disease or peripheral arterial disease who were enrolled in a clinical trial. Patients were not taking any other antiplatelet or anticoagulant drugs. We measured light transmission aggregometry (LTA) with 1.5mM arachidonic acid (AA), and 5 and 10 uM ADP; VerifyNow Aspirin (Elitech UK); activation markers, P-selectin expression and fibrinogen binding by whole blood flow cytometry; plasma fibrinogen by Clauss clotting assay; and vWF antigen by ELISA.

Results AA-induced aggregation ranged from 0 to 12% maximum (median 4%), and 99% of patients exhibited a good response to aspirin with this direct test of cyclooxygenase activity. When ADP was used as agonist, 8% of patients were above the reported 70% aggregation cut-off for "poor responders" with 5uM ADP, and 22% with 10uM ADP. Using VerifyNow Aspirin, only one patient's result was above the manufacturers' threshold for incomplete response to aspirin. Significant correlations were found between AA-LTA and ADP-LTA and Verify Now Aspirin, but not with any of the other platelet tests. There were significant positive correlations between LTA and plasma vWF (AA-LTA $r=0.35$ $p=0.012$; 5ADP $r=0.45$ $p=0.001$; 10ADP $r=0.37$ $p=0.009$), but not with plasma fibrinogen.

Conclusion Platelet responsiveness to arachidonic acid was effectively inhibited by aspirin in almost all patients. Predictably, there was more variability in response to ADP, probably due to platelet activation through non-aspirin-dependent pathways. Platelet activation markers did not reflect the aspirin response. These results support the use of the point-of-care test, VerifyNow Aspirin as it correlated well with AA-LTA, is simpler and faster to perform, and was not affected by vWF or fibrinogen levels.

P24

MitoSNO1 as a potential therapeutic in experimental stroke

Danyele Carr^{1*}, Katie Y. Hood^{1*}, Emily N.J. Ord¹, Mike P. Murphy², Lorraine M. Work¹

1: BHF GCRC, ICAMS, University of Glasgow, Glasgow, G12 8TA

2: Mitochondrial Biology Unit, University of Cambridge, Cambridge, CB2 0XY

*These authors contributed equally to this study

Mitochondria are a major site of reactive oxygen species production and protecting mitochondria from oxidative damage may be an effective strategy in ischaemic stroke. The mitochondrial targeted S-nitrosothiol, MitoSNO1, is protective following cardiac ischaemia *ex vivo*¹. We aimed to determine if such protection could be achieved *in vitro* in rat neuronal (B50) and cerebral endothelial (GPNT) cells following hypoxia/reoxygenation (H/R) and *in vivo* after cerebral ischaemia in spontaneously hypertensive stroke prone rats (SHRSP).

Cells were exposed to 9 hours hypoxia (1% O₂, 5% CO₂, balance N₂) and 24 hours reoxygenation ± MitoSNO1, MitoNAP or SNAP administration (1µM or 5µM) before determination of superoxide levels (electron paramagnetic resonance, EPR), lipid peroxidation (malondialdehyde, MDA, assay) or apoptosis (caspase 3 immunocytochemistry, ICC). Male, 16 week old SHRSP were randomly assigned to one of 3 treatment groups (200 ng/kg MitoSNO1 or MitoNAP or saline) and subjected to transient middle cerebral artery occlusion (tMCAO, 45 mins). Post-stroke recovery was assessed using a 32-point neurological score and the tapered beam walk test. Infarct volume was determined following sacrifice (+3 days from tMCAO) by triphenyltetrazolium chloride (TTC) staining. The MDA assay was performed on brain homogenates (ipsilateral and contralateral hemispheres) as a measure of lipid peroxidation.

H/R resulted in a significant increase in levels of superoxide measured by EPR, lipid peroxidation determined by an MDA assay (p<0.05 vs normoxic controls) and an alteration in both the amount and cellular location of caspase 3 protein by ICC in B50 and GPNT cells. This was completely prevented by treatment with MitoSNO1 during reoxygenation whereas no such protection was seen with control compounds (MitoNAP or SNAP). In SHRSP, intra-arterial administration of MitoSNO1 upon reperfusion significantly reduced infarct volume determined 3 days post-tMCAO while MitoNAP had no such effect. Measures of neurological deficit further demonstrated a trend to an improvement in neurological outcome in those animals randomised to receive MitoSNO1 compared to tMCAO control and tMCAO + MitoNAP. Furthermore, survival in the MitoSNO1 treated group was 100% compared to 66% after tMCAO and 72% in tMCAO + MitoNAP.

MitoSNO1 delivery during reoxygenation protects neuronal and cerebral endothelial cells following hypoxia. Furthermore, intra-arterial delivery of MitoSNO1 on reperfusion following tMCAO led to reduced infarct volume. These findings demonstrate the potential for mitochondrial targeted NO donors as a novel therapeutic for stroke.

¹Prime *et al* (2009), *Proc Natl Acad Sci USA*, **106** 10764-10769.

P25

Comparing the haemodynamic differences in the outflow of vascular prostheses

Kokkalis E^{1,5}, Hoskins PR², Corner GA³, Doull AJ⁴, Stonebridge PA⁵, Houston JG⁵

1: *Institute for Medical Science and Technology, University of Dundee, Dundee*

2: *Centre for Cardiovascular Science, University of Dundee, Dundee*

3: *Medical Physics, Ninewells Hospital and Medical School, Dundee*

4: *School of Computing, University of Dundee, Dundee*

5: *Division of Cardiovascular Research, Ninewells Hospital and Medical School, Dundee*

Background and Objectives

Vascular grafts are widely used to treat peripheral vascular disease and for vascular access in patients requiring dialysis. Their patency rates remain a challenge, with restenosis in the distal anastomosis to be a common reason of failure. The blood flow profile is considered as a crucial factor for endothelial function and the formation of neointimal hyperplasia. Spiral flow is known to be a normal feature of the arterial system induced by anatomical structure and physiological function. This study compared flow patterns created by vascular prostheses specifically engineering to induce single spiral flow against standard grafts, using an *in vitro* setup.

Methods

*Spiral Laminar Flow*TM Peripheral Vascular (PV) and Access Vascular (AV) grafts (Vascular Flow Technologies, UK) were compared with control PV and AV grafts respectively. The flow phantom was consisted by a piston pump (Shelley Medicals, Canada), blood mimic (ATS, USA) and vessel mimicking tubing (15% PVA-cryogel) in 9% glycerol solution. Steady flow rates of up to 720 ml/min were applied. A HDI 5000 ultrasound scanner was used for colour Doppler data collection at the cross-sectional view distally from the grafts outflow. A vector Doppler imaging technique was developed to detect rotational patterns in the outflow of the prostheses, using MatLab (MathWorks, USA). Two-dimensional radial velocity magnitude and directional maps were created. For both sets of grafts the velocity magnitudes were compared.

Results and Conclusions

The *Spiral Laminar Flow*TM grafts were able to produce a single spiral pattern in their

outflow associated with flow coherence. Two or more spirals were detected in the outflow of the control devices with the phenomenon to be more disturbed in the proximal outflow. These complicated secondary flow motions were related to flow separation. The quality of the joining connection between the spiral grafts and the vessel mimic was an important factor for the resulting outflow pattern. The radial velocity was found to be higher for the single spiral flow in comparison to the more complicated rotational patterns for a range of applied flow rates. It is expected that the magnitude of radial velocity proportionally affects wall shear stress. The clinical significance of these flow patterns is yet to be established. However, these results support the hypothesis that spiral grafts can introduce flow stability and increase wall shear stress, which are believed to inhibit restenosis.

P26

Beneficial effects of an aromatase inhibitor in two distinct models of established pulmonary arterial hypertension.

KM Mair¹, N Duggan², D Rowlands², M Hussey², S Roberts², J Fullerton¹, M Nilsen¹, M Thomas², MR. MacLean¹.

1: *Institute of Cardiovascular and Medical Science, MVLS, University of Glasgow, Glasgow, UK.*

2: *Novartis Pharmaceuticals UK Limited, Horsham Research Centre, West Sussex, UK*

Rationale: The role of estrogen in the pathobiology of pulmonary arterial hypertension (PAH) remains controversial, with both protective and pathogenic effects of the sex hormone described. Furthermore, little is known about the role of aromatase, the enzyme responsible for estrogen synthesis, in the disease process. Here we assess the role of aromatase and estrogen in two distinct models of PAH using the clinically available aromatase inhibitor anastrozole.

Methods: The role of aromatase in PAH was investigated using a hypoxic murine model, and the rat hypoxic/SUGEN model of the condition. Female mice were exposed to hypobaric hypoxia for 14 days in order to establish a PAH phenotype. These animals were then maintained in hypoxia for a further 14 days with concurrent administration of anastrozole (3mg/kg/day). Similarly, female rats were administered with SUGEN 20mg/kg and maintained in hypoxic conditions for 14 days. The rats were then maintained in normoxic conditions for a further 14 days with concurrent administration of anastrozole (3mg/kg/day). Aromatase immuno-reactivity was also assessed in human lung sections from control and pulmonary hypertensive patients.

Results: In the hypoxic mouse study anastrozole was found to significantly reduce hypoxia-induced elevations in sRVP (32.41 ± 2.0 mmHg *versus* 41.76 ± 1.3 mmHg; $p < 0.001$). Additionally, similar reductions were also observed on hypoxia-induced RVH (RV/LV+S: 0.38 ± 0 *versus* 0.44 ± 0.02 ; $n \geq 8$; $p < 0.01$) and pulmonary vascular remodelling. Anastrozole had no effect on pulmonary hemodynamics under normoxic conditions nor did it have any significant effect on systemic arterial pressure or heart rate. Anastrozole also significantly attenuated the elevated RVH ($p < 0.001$; $n = 8$) and the % of muscularised vessels ($p < 0.05$; $n = 8$) observed in the hypoxic/SUGEN rat model. Furthermore, immuno-histochemical analysis revealed aromatase is highly expressed in pulmonary arteries of both control and PAH patients, where it is localised mainly within the vascular smooth muscle.

Conclusions: Taken together these findings provide further evidence that estrogen plays a pathogenic role in the development of PAH, as inhibition of estrogen synthesis using anastrozole prevents the progression of the condition in two distinct rodent models of established disease. We also demonstrate that aromatase is expressed in pulmonary artery smooth muscle in humans, suggesting the occurrence of localised estrogen production in the pulmonary artery.

P27

Aspirin-induced inhibition of platelet aggregation and eicosanoid metabolism: more than just an inhibitor of cyclooxygenase?

Maskrey BH¹, Rushworth GF², Law MH¹, Wei J¹, Leslie SJ^{1,3}, Whitfield PD¹, Megson IL¹

¹Department of Diabetes & Cardiovascular Science, University of the Highlands & Islands, Inverness, UK, IV2 3JH.

²Highland Clinical Research Facility, Centre for Health Science, Inverness, UK

³Cardiac Centre, NHS Highland, Raigmore Hospital, UK

The established mechanism by which aspirin induces inhibition of platelet aggregation is that it inhibits platelet cyclooxygenase-1 (COX-1), blocking formation of the potent platelet activator, thromboxane A₂ (TXA₂). However, it has long been recognised that the effect of aspirin might extend beyond selective COX inhibition. In this pilot study, we evaluated the impact of *in vivo* administration of a standard antiplatelet dose (75 mg) aspirin in 19 healthy volunteers on the acute (t=1.5 h) impact of *in vitro* platelet aggregation and on eicosanoids generated by the COX and lipoxygenase (LOX) pathways. The results indicate that, whilst aspirin-induced inhibition of thromboxane B₂ (TXB₂) generation was consistently robust amongst the study population, the extent of aspirin inhibition on platelet aggregation varied widely. Indeed, the variation in sensitivity of platelets to aspirin inhibition was more closely associated with inhibition of LOX-derived 12-hydroxyeicosatetraenoic acid (HETE) than COX-derived TXB₂. These findings question the paradigm that the anti-platelet effects of aspirin are exclusively mediated via COX inhibition and lend weight to the concept that inhibition of 12-HETE might be an important determinant of platelet sensitivity to aspirin. Further research is merited to determine the role of 12-HETE in platelet activation and establish whether this ineffective and variable inhibition of LOX plays a role in so-called aspirin resistance.

P28

High variability in peak signal intensity and contrast dynamics during first pass

perfusion imaging: a CMRI study

Shona Matthew PhD¹, Deirdre Cassidy BSc Hon², Stephen Gandy PhD¹, J Graeme Houston FRCP, FRCR¹

1: Cardiovascular & Diabetes Imaging, University of Dundee, Dundee, Angus, United Kingdom, 2: NHS Tayside Medical Physics, Dundee, Angus, United Kingdom, 3: NHS Tayside Clinical Radiology, Dundee, Angus, United Kingdom.

Introduction Cardiac magnetic resonance (CMR) first-pass perfusion imaging (FPPI) plays a central role in the diagnosis, clinical management and prognosis of patients with known or suspected ischemic heart disease. During FPPI, a bolus of contrast agent is dynamically tracked as it passes through the chambers of the heart and into the myocardium, providing a non-invasive, non-ionising method of assessing and quantifying coronary microcirculation. This study sought to provide a semi-quantitative analysis of FPP data, focusing on the dose/kg, bolus transit time (TT), peak signal intensity (PSI) in the left ventricular blood pool (LVBP), and myocardium, patient heart rate (HR), ejection fraction (EF) and left ventricular mass (LVM) in order to determine the natural variability in contrast dynamics in a randomly selected cohort of volunteers.

Method and Materials Thirty eight volunteers: 19 males (M), mean age and (50: 14-78) years and 19 females (F), mean age and range (52: 16-78) years were selected from a database of individuals referred for FPP imaging at 1.5T (Avanto, Siemens, Erlangen, Germany). Image analysis was performed on a Siemens multi-modality work station using ARGUS software (version VB15).

Results and Discussion A 20ml dose of contrast agent (Gadoteric Acid, Guerbet, France) was administered to each volunteer rather than the standard 0.2ml/Kg. Hence, individual doses varied from > 0.40 ml/Kg to < 0.20 ml/Kg depending on body mass index (BMI). Dose/kg bore no correlation to the TT of the bolus from the injection site to the LVBP or myocardium, or on the PSI in the LVBP or myocardium. Similarly, the EF and HR of volunteers did not impact on the TT of the bolus through the chambers of the heart (from the right atrium to the left ventricle), the arrival time of the bolus in the LV or the PSI detected in the BP or myocardium at first pass. PSI in the LVBP did correlate strongly with PSI in the myocardium during FPP.

Conclusion Peak signal intensity in the LVBP correlates strongly with PSI in the myocardium during FPP but does not correlate with volunteer HR, EF, LVM or the administered dose/Kg of contrast agent. In addition, the contrast agent dose/Kg does not correlate with the TT of the bolus from the RA to the LV of the heart or the arrival time of the bolus in the LV. This high variability in myocardial signal intensity and contrast agent dynamics between individuals needs to be recognised in the interpretation of these examinations as it does not appear possible to control for this variability on the basis of LV parameters or contrast agent dose/kg alone.

P29

Intra and inter-observer variability in whole-body contrast enhanced MRA stenosis grading and systemic atheroma scoring

L McCormick¹, J Weir-McCall², RD White², JJ Belch³, SJ Gandy⁴ AD Struthers⁵, F Sullivan⁶, R Littleford¹, JG Houston^{1,2}

1: The Institute of Cardiovascular Research, Division of Medical Sciences, University of Dundee, Dundee

2: Clinical Radiology, NHS Tayside Academic Health Sciences Centre, Ninewells Hospital, Dundee,

3. Division of Cardiovascular and Diabetes Medicine, Ninewells Hospital, Dundee

4. Medical Physics, NHS Tayside Academic Health Sciences, Ninewells Hospital Dundee

5. Department of Clinical Pharmacology and Therapeutics, University of Dundee, Dundee

6. Division of Population Health Sciences, University of Dundee, Dundee

Aim: To determine the reproducibility of two radiologists in whole-body contrast-enhanced MRA cardiovascular analysis.

Methods: 20 patients (11 male, 9 female, age range 58-77 years), with 5 patients in each subgroup of healthy, mild, moderate and severe atheroma burden, were imaged on a 3.0 Tesla MRI scanner (Magnetom Trio, Siemens, Erlangen, Germany). Coronal FLASH sequences were used to obtain contrast-enhanced MR angiograms of each patient. Two cardiovascular radiologists performed manual stenosis analysis on 159 arterial sites in each of these patients. A categorical stenosis grading scale was applied to each of these sites. Whole-body atheroma scores were calculated as a summation of all assigned grades, normalised for interpretable sites.

Results: The reproducibility of each observer's analysis was substantial in the analysis of the moderate and severe symptomatic patients groups (Observer 1 Kappa (k)=0.603 \pm 0.029 moderate, k = 0.582 \pm 0.024 severe; Observer 2 k = 0.559 \pm 0.031 moderate , k = 0.626 \pm 0.023 severe; P <0.001), but only fair in the grading of the healthy and mild atherosclerosis patients' groups (Observer 1 k = 0.404 \pm 0.057 healthy, k = 0.501 \pm 0.029 mild, Observer 2 k = 0.391 \pm 0.061 healthy, k = 0.432 \pm 0.034 mild, P <0.001). Correlation between radiologist whole-body atheroma scoring was high (Spearman correlation = 0.911, P <0.01).

Conclusions: Observer reproducibility and agreement was moderate to substantial in the grading of clinically significant stenosis. Observer disagreement associated with the grading of minor pathologies does not reduce high consensus in whole-body atheroma scoring.

P30

MicroRNA analysis in experimental models of vein graft neointima formation identifies a critical role for miR-21 in neointima formation.

McDonald RA¹, White KM^{1*}, Wu J^{2*}, Robertson KE¹, Cooley BC³, Halliday C¹, Lu R¹, Hu J⁴, Kennedy S¹, Wadsworth RM², George SJ⁵, Wan S⁴, Baker AH¹.

¹Institute of Cardiovascular and Medical Sciences, University of Glasgow, Glasgow, UK.

²Strathclyde Institute of Pharmacy and Biomedical Sciences, University of Strathclyde, Glasgow. ³Allen Bradley Medical Sciences Laboratory, Medical College of Wisconsin.

⁴Division of Cardiothoracic Surgery, Prince of Wales Hospital, The Chinese University of Hong Kong, Hong Kong, China. ⁵Bristol Heart Institute, School of Clinical Sciences, Bristol Royal Infirmary, Upper Maudlin St, Bristol. * indicates equal contributions.

Background: Coronary artery bypass grafting (CABG) is an established treatment to relieve the symptoms of ischemic heart disease. However premature graft failure, in saphenous veins is a major limitation. One of the principal etiological factors responsible for vein graft failure is activation and phenotypic modulation of smooth muscle cells (SMC), resulting in accelerated rates of proliferation and migration. MicroRNAs (miRNAs) are short, single stranded, non-coding RNAs that play important roles in modulating cell phenotypes through regulation of gene expression.

Methods & Results: In order to assess the expression levels of miR-21 in the progression of vein graft neointimal formation, we quantified miR-21 levels in three well-established models of vein graft disease. These were the *in vivo* porcine model of interposition graft, the isogenic mouse model, as well as the *ex vivo* human saphenous vein model of neointimal formation. MiR-21 levels were up-regulated approximately 7-fold in both the porcine and murine models at 7 and 28 days following grafting (n=6). In surgically prepared Human saphenous veins (HSV) which were subjected to culture *ex vivo* we found that miR-21 levels were elevated approximately 3-fold following 7 and 14 days of culture (n=6). In situ localization in the HSV demonstrated that miR-21 was expressed most intensely in the neointimal layer of HSV which also stained positive for SMC actin. Co-localization studies in murine vein grafts revealed that miR-21 was localised to areas of the graft that stained positive for proliferating cell nuclear antigen with substantial co-staining with SMC actin. We assessed the potential functional role of miR-21 in vein graft failure using miR-21 knockout mice. Analysis of neointimal lesion size in miR-21 knockout mice revealed an 81% reduction in neointimal area compared to wild type controls ($p \leq 0.0001$, n=7-10/group). Furthermore, pharmacological inhibition of miR-21 in human saphenous veins resulted in target gene de-repression and a significant reduction in neointimal formation.

Conclusion: These findings demonstrate that miR-21 is up-regulated in multiple models of vein graft disease and that genetic abolition of miR-21 levels can attenuate neointimal formation in response to grafting. Therein, modulation of miR-21 expression represents a novel therapeutic opportunity in the setting of vein graft neointimal formation.

P31

A combined gene-therapy and pharmacological intervention protects from cerebral ischaemia *in vivo* and hypoxia / reoxygenation *in vitro*.

E. N. J. Ord¹, R. Shirley¹, C. McCabe², E. J. Kremer³, I. M. Macrae² & L. M. Work¹

¹Institute of Cardiovascular and Medical Science or ²Institute of Neuroscience and Psychology, College of Medical, Veterinary and Life Sciences, University of Glasgow, UK.

³IGMM CNRS, UMR 5535, 34293 Montpellier, France.

Stroke remains the 3rd leading cause of death in the UK with <5% of patients receiving therapeutic thrombolysis. We propose by combined neuroglobin (Ngb) overexpression and JNK inhibition, using gene- and drug-delivery, a greater beneficial effect than either agent alone will be seen in an *in vitro* proof-of-concept study and subsequently in a robust preclinical experimental stroke model. Lentivirus-mediated Ngb overexpression (5 vp/cell) combined with JNK inhibition (SP600125, 20 μ M) significantly reduced oxidative stress following 9 hrs hypoxia/24 hrs reoxygenation in rat neuronal (B50) cells determined by electron paramagnetic resonance (normoxic 551 \pm 6, hypoxic 838 \pm 30, combined 571 \pm 11* counts/min/ng protein *p=0.001 vs. hypoxic) and malondialdehyde assay (normoxic 0.365 \pm 0.03, hypoxic 1.369 \pm 0.12, combined 0.359 \pm 0.03* MDA μ mol/ μ g protein *p=0.0002 vs. hypoxic). Treatment also significantly reduced apoptosis assessed by cell death ELISA (normoxic 0.103 \pm 0.004, hypoxic 0.302 \pm 0.006, combined 0.108 \pm 0.006* absorbance/ μ g protein *p<0.005 vs. hypoxic) and immunostaining for nuclear-localised caspase 3. Male SHRSPs were subjected to transient middle cerebral artery occlusion (tMCAO) ((5 groups, n=9) tMCAO; control green fluorescent protein-expressing canine adenovirus, CAV-GFP; Ngb-expressing CAV, CAV-Ngb; SP600125, 1 mg/kg *i.v.*; CAV-Ngb+SP600125) or sham procedure and longitudinally assessed for neurological outcome (+14 days) before infarct determination. CAV (3x10⁹ vp) was administered stereotactically into the cortex 5 days pre-tMCAO. Infarct volume was significantly decreased from tMCAO (324.12 \pm 16.4 mm³) and control virus (313.88 \pm 22.2 mm³) groups by pretreatment with either CAV-Ngb (198.96 \pm 14.4 mm³, *p<0.01 vs. control) or SP600125 (214.82 \pm 35.2 mm³, *p<0.01 vs. control) treatment alone, but further significantly improved by CAV-Ngb+SP600125 (137 \pm 20.7 mm³, †p<0.01 vs. SP600125). Neurological outcome was significantly improved in CAV-Ngb and SP600125 groups, and further significantly improved by CAV Ngb+SP600125 combined treatment. Upregulation of Ngb by CAV was maintained 19-post injection assessed semi-quantitatively by immunocytochemistry. Our translational study demonstrates combined Ngb overexpression with JNK inhibition improves neurological outcome greater than either therapy alone *in vitro* following hypoxia / reoxygenation and *in vivo* following transient cerebral ischaemia.

P32

Lipidome profile of human LDL: finding out the best extraction solvent system

Ana Reis¹, Alisa Rudnitskaya², Gavin Blackburn³, Andy Pitt¹, Corinne Spickett¹

1: School of Life and Health Sciences, Aston University, Birmingham, UK

2: CESAM, Universidade de Aveiro, Aveiro, Portugal

3: Strathclyde Institute of Pharmacy and Biomedical Sciences, Glasgow, UK

Lipids have a plethora of bioactivities and signalling functions in addition to structural roles. To explore the role of lipids in health and disease, the profiling and identification of lipids have become fundamental, with mass spectrometry (MS) as the main method of choice. However, the success of lipidomic studies for any given sample (tissue, cell or fluid) is critically dependent on the efficiency of the extraction step, which ideally should effectively extract lipids representative of the sample without bias, prevent degradation of lipids, and minimise contamination by non-lipid components. The performance of a particular solvent system depends on the partitioning of the different lipid classes into the organic phase, and consequently on the sample lipid composition. Recently, to replace the environmental harmful chlorinated solvents, alternative solvent systems have been proposed and reported to have similar efficiencies in the extraction of predominant lipid species when compared to existing protocols. Despite this, pairwise comparisons are limited to predominant classes and do not provide broader analysis of minor lipid classes.

In this study, 5 solvent systems were compared for the lipid extraction in LDL from pooled plasma of healthy individuals. Lipids extracted were analysed by normal-phase chromatography using HILIC mode, detected using a high resolution instrument with dual polarity (Exactive, Thermo Scientific, Hemel Hempstead, UK). Chromatograms were aligned and the features (ions) extracted with XCMS online software (Scripps Center for Metabolomics, USA) and processed using ANOVA-Simultaneous Component Analysis (ASCA) to assess the effects of the solvent systems on the extraction of lipids. Statistical significance was evaluated using a permutation test with 1000 permutations. In total more than 350 lipid species from 19 different lipid sub-classes were identified from LDL, increasing the lipidome coverage described so far, with lipoamino acids (LAA) being reported for the first time. Evaluation performed on 10 lipid classes showed little differences in the extraction of predominant lipid classes (TAG and CE) between the 5 systems, but significant differences in minor and low abundant lipid classes (lyso-PC, PI, PE, LAA, CS, and LacCer). Based on these findings, an optimum solvent system for the extraction of wide range of lipid classes from LDL is recommended for the implementation of lipidome analysis on a routine basis.

This research was supported by a Marie Curie Intra-European Fellowship within the 7th European Community Framework Program (IEF 255076). Work of A. Rudnitskaya was supported by Portuguese Science and Technology Foundation, through the European Social Fund (ESF) and "Programa Operacional Potencial Humano – POPH. GB acknowledges support from the "Scottish University Life Sciences Alliance for funding and that all mass spectrometry analysis was carried out at ScotMet: The Scottish Metabolomics Facility."

P33

The Role of Sodium Channels Present on the Rat Pulmonary Vein in the Generation of Arrhythmogenic Activity in Atrial Fibrillation

Laura Hutchison¹, Andrew Rankin², Robert Drummond¹, Edward Rowan¹

1: Strathclyde Institute of Pharmacy and Biomedical Sciences, University of Strathclyde, Glasgow, UK.

2: School of Medicine, University of Glasgow, Glasgow, UK.

Atrial fibrillation is the most common cardiac arrhythmia, currently affecting 1% to 1.5% of the developed world population and is a significant cause of morbidity and mortality. This arrhythmia is characterised by uncoordinated and disorganized contraction of the atria. Clinical studies in atrial fibrillation patients have demonstrated ectopic foci can originate from the pulmonary veins with the external sleeve of cardiomyocytes surrounding the pulmonary veins believed to be responsible for the veins arrhythmogenic susceptibility (Haissaguerre *et al.*, 1998). Alterations in the sodium current in atrial cardiomyocytes are potentially arrhythmogenic. Sossalla *et al.*, 2010 demonstrated a sustained sodium current in atrial cardiomyocytes of atrial fibrillation patients resulted in arrhythmogenic early after depolarisations. However the exact mechanism and the key sodium current alternations in atrial and pulmonary vein cardiomyocytes remain unclear. The aim of this study was to determine the presence and localisation on cardiomyocytes of the Tetrodotoxin (TTX)-insensitive, Na_v1.5 and TTX-sensitive sodium channels and explore their contribution in pulmonary vein arrhythmogenesis.

Reverse Transcription-PCR with rat pulmonary vein, atrial and ventricular preparations confirmed the presence of specific TTX-sensitive and TTX-insensitive sodium channels. Immunofluorescence was then utilised to demonstrate the localisation of sodium channels along the membrane of rat pulmonary vein cardiomyocytes. Sharp microelectrode electrophysiology studies on intact pulmonary veins with nM concentrations of TTX to block TTX-sensitive sodium channels and μ M concentrations of TTX to block TTX-insensitive sodium channels demonstrated the effect of sodium channel blockade on the pulmonary vein cardiomyocyte action potential.

Further functional studies are now needed in order gain further insight on the arrhythmogenic properties of the presence, absence or mutations of the sodium channels of atrial and pulmonary vein cardiomyocytes and establish if there is a link between this and atrial fibrillation.

Haissaguerre M, Jais P, C. Shah D, Takahashi A, Hocini M, Quiniou G, Garrigue S, Le Mouroux A, Le Metayer P and Clementy J (1998) Spontaneous Initiation of Atrial Fibrillation By Ectopic Beats Originating In The Pulmonary Veins. *N Engl J Med*, **339**: 659-666.

Sossalla S, Kallmeyer B, Wagner S, Mazur M, Maurer U, Toischer K, Schmitto JD, Seipelt R, Schöndube FA, Hasenfuss G, Belardinelli L and Maier LS (2010) Altered Na⁺ Currents in Atrial Fibrillation: Effects of Ranolazine on Arrhythmias and Contractility in Human Atrial Myocardium. *JACC*, **55**:2330-2342

P34

Polyphenol-rich foods intake reduces CVD risk factors in healthy volunteers

E A S Al-Dujaili¹, C Tsang², S Almoosawi³, J Hall¹, I Davidson¹, L Fyfe¹

1: Dietetics, Nutrition and Biological Sciences, School of Health Sciences, Queen Margaret University, Edinburgh, UK

*2: Health & Food Science, School of Contemporary Sciences
University of Abertay Dundee*

*3: MRC Human Nutrition Research, Elsie Widdowson Laboratory,
120 Fulbourn Road, Cambridge CB1 9NL, UK*

Epidemiological studies suggest that diets high in polyphenols may have a protective effect against oxidative stress and play a critical role in the prevention of some common diseases such as hypertension, diabetes and obesity^{1,2}. However, the diversity and complexity of these compounds implies that much remains to be elucidated concerning the mechanisms by which these compounds influence health. We have recently reported that dark chocolate consumption (Barry Calbout, Belgium) can reduce fasting blood glucose levels, systolic and diastolic blood pressure³. The effects of green coffee bean extract, green tea and grape juice on blood pressure and glucocorticoids were investigated and compared in healthy volunteers of different age, gender and BMI.

Participants were asked to consume the polyphenol-rich food for 2 weeks, and saliva and 24h urine samples were collected before and after the intervention. Total phenolics, antioxidant capacity and glucocorticoids (cortisol and cortisone) were measured. Green coffee bean extract (90mg chlorogenic acid per day) decreased systolic blood pressure from 119.4±10.5 to 113.8±9.1 mmHg (p=0.05). Green tea (4 cups per day) significantly reduced systolic blood pressure by 7.1mmHg (p<0.001) and diastolic blood pressure by 4.8mmHg over 14 days (p<0.01). However, dark grape juice consumption (0.5L/day) did not influence blood pressure. In addition, green tea consumption reduced mean fasting total cholesterol by 0.556 mmol/L (p<0.008), BMI by 0.34 kg/m² (p<0.01), body weight by 0.96 kg (p<0.01) and body fat mass by 2.36% (p<0.05). No changes were detected in BMI or body weight following green coffee bean extract or grape juice. Following green coffee bean extract consumption urinary 24h free cortisol was reduced from 1.0523 to 0.763±0.40nmol/kg (p=0.07). Free cortisone excretion was increased from 0.712±0.38 to 0.932±0.24 nmol/kg (p=0.007), and the ratio of cortisol/cortisone was reduced (from 1.48±0.65 to 0.82±0.42, p=0.03). All 3 products tested produced an increase in urinary total phenolics (p=0.003) and antioxidant capacity (p<0.001). Dark grape juice intake by exercisers and sedentary groups indicated that urinary basal antioxidant capacity was found to be significantly lower in the latter compared to exercisers (p=0.05), and that exercisers had a slight but significant increase in antioxidant capacity (p=0.05) following grape juice consumption. In conclusion, our results suggest that consumption of polyphenol-rich foods may offer potential protection against hypertension, diabetes and obesity-related complications, and the reduction in blood pressure may be due to the modulation of glucocorticoids levels.

1. Arts ICW, Hollman PCH. (2005) Polyphenols and disease risk in epidemiologic studies. *Am J Clin Nut.* 81 (suppl): 317S-325S.

2. Geleijnse JM, Hollman PCH (2008) Flavonoids and cardiovascular health: which compounds, what mechanisms? *Am J Clin Nut.* Vol 88: 12-13.

3. Almoosawi S, C. Tsang, L. M. Ostertag, L. Fyfe and E. A. S. Al-Dujaili (2012) Differential effect of polyphenol-rich dark chocolate on biomarkers of glucose metabolism and cardiovascular risk factors in healthy, overweight and obese subjects: a randomized clinical trial. *Food Function*, 2012, 3, 1035.

P35

GLP-1 peptides attenuate agonist-induced hypertrophy in H9c2 cardiomyocytes

Sam Lockhart, Adam P Harvey, Emma Robinson, Declan McLaughlin, Kerry Burch, David Grieve.

Queen's University Belfast, Centre for Vision and Vascular Science, School of Medicine, Dentistry and Biomedical Sciences, Grosvenor Road, Belfast BT12 6BA

Introduction: GLP-1 is an incretin hormone that has been exploited therapeutically in the treatment of type 2 diabetes. Interestingly, it has emerging beneficial actions in experimental and clinical chronic heart failure (CHF). Furthermore, its metabolite, GLP-1 (9-36), has cardioregulatory actions. However, its actions in the setting of CHF have not yet been delineated. Here, we assessed the ability of native GLP-1, the mimetic exendin-4 (Ex-4) and metabolite GLP-1(9-36) to modulate specific components of chronic cardiac remodelling *in vitro*.

Methods: Cardiomyocyte hypertrophy and apoptosis were assessed independently in H9c2 and HL-1 cardiomyocytes following pre-treatment with GLP-1 peptides (0.1 $\mu\text{mol/L}$). Cardiomyocyte hypertrophy was induced with phenylephrine (PE) treatment (10 $\mu\text{mol/L}$ for 96 hours) and quantitatively assessed using digital image analysis. Activated caspase 3/7 was measured as an endpoint of cardiomyocyte apoptosis following doxorubicin treatment (5 $\mu\text{mol/L}$ for 24 hours). The MEK-1 inhibitor, PD98059 (50 $\mu\text{mol/L}$), and the PI3K inhibitor wortmannin (WM, 0.1 $\mu\text{mol/L}$) were used to assess the role of candidate signaling molecules.

Results: Phenylephrine (PE)-induced H9c2 cardiomyocyte hypertrophy was attenuated by both GLP-1 and Ex-4 (PE: 1.39 \pm 0.10 vs PE Ex-4: 1.11 \pm 0.05 arbitrary units, $n=4$; $P<0.05$). GLP-1(9-36) treatment also reduced cardiomyocyte area, but this was not statistically significant (PE:1.39 \pm 0.10 vs PE Ex-4: 1.23 \pm 0.08 arbitrary units, $n=4$; $P = \text{NS}$). The protective actions of Ex-4 were abolished by WM treatment (PE WM:1.32 \pm 0.03 vs PE Ex-4 WM:1.40 \pm 0.12 arbitrary units; $n=4$, $P=\text{NS}$). In contrast, doxorubicin-induced apoptosis of HL-1 cardiomyocytes was unaffected by GLP-1 treatment.

Implications: GLP-1 may exert differential actions on component processes of cardiac remodeling, which may underlie its beneficial actions in CHF. The role of its metabolite GLP-1(9-36) is still unclear, however, our data suggest that it may have some anti-hypertrophic activity. This could have important implications for experimental design in future studies investigating the role of GLP-1 in CHF.

P36

Sex Differences in Vascular Endothelial Cell Function Reveal a Gender Specific Role for Nitroxyl

Kayleigh Hamilton and Andrew MacKenzie

Institute of Biomedical and Environmental Health Research, University of the West of Scotland

Nitric oxide (NO; which plays a critical role in vascular health) is produced by eNOS in endothelial cells (EC) and activates soluble guanylate cyclase (sGC) to induce vasorelaxation. NO can also exist as the vasorelaxant nitroxyl (HNO) although the precise role for this form is not fully understood. Given that gender-specific variations exist in vascular activity we investigated if HNO generation underlies any differences between the sexes.

Using isolated rings of aorta from female (n=16) and male (n=20) Sprague Dawley rats, and following sub-maximal contraction with phenylephrine (PE), responses to ACh (1nM - 3µM) were measured isometrically in EC-containing or –denuded rings with and without a range of pharmacological inhibitors. In separate experiments, the depression of PE (1nM - 3µM)-induced contraction was used as a measure of the tonic vasodepressor influence of the EC in the absence of ACh. Data are given as means ± SEM, compared by ANOVA, n≥6 for all observations.

In aortic rings from both females and males, ACh-induced EC-dependent relaxation was completely abolished following incubation with either L-NAME (300µM; P<0.001), hydroxocobalamin (100µM; P<0.001) or ODQ (30nM; P<0.001) suggesting that the relaxation was dependant entirely on eNOS activity, generation of NO and sGC activation, respectively. As determined by the depression of PE-induced contraction, the tonic vasodepressor influence of the EC in aortic rings from females was shown to be completely reliant on eNOS, the NO radical and sGC activation (i.e. treatment with L-NAME, hydroxocobalamin and ODQ, respectively, altered PE-induced contraction so that it was indistinguishable from EC-denuded vessels, P>0.05). In aorta from males, EC-dependant depression of PE (max contraction in EC-containing rings was 1.0±0.3g vs. 2.0±0.2g in EC-denuded preparations; P<0.001) was also shown to be eNOS and sGC dependant (contraction in L-NAME and ODQ treated tissue was 1.9±0.1g and 2.1±0.2g, respectively; neither statistically different from EC-denuded rings, P>0.05). However, in powerful contrast to females, inactivation of NO with hydroxocobalamin only partly impaired the influence of EC (1.6±0.2g; P<0.01 compared to EC-denuded rings) suggesting the presence of a non-NO mediator. Use of the established HNO scavenger L-cysteine (3mM) produced a partial inhibition of the vasodepressor influence of EC (1.5±0.1g; P<0.05 compared to EC-containing rings) but in combination with hydroxocobalamin produced an effect greater than when either was used independently (1.9±0.2g; indistinguishable from EC-denuded rings, P>0.05).

In conclusion, tonically active eNOS in aortic EC from male, but not female, rats generate both NO and HNO but the HNO contribution is lost when the EC are stimulated by ACh. These data identify a gender specific role for HNO.

P37

Imaging the healing murine myocardial infarct *in vivo*: ultrasound, MRI and fluorescence molecular tomography

Gillian A Gray, Adrian Thomson, Christopher I White, Ian Marshall, Carmel Moran & Maurits Jansen

Centre for Cardiovascular Science & Edinburgh Preclinical Imaging, Queens Medical Research Institute, University of Edinburgh.

Improved understanding of the processes involved in myocardial infarct healing is required for identification of novel therapeutic targets to limit infarct expansion and consequent long term ventricular remodeling after myocardial infarction (MI). Infarction can be modeled effectively in murine models of coronary artery ligation. The best experimental design will allow interrogation of early ischaemic injury and infarct healing processes, as well as development of structural and functional alterations during chronic remodelling, in a longitudinal study. The murine heart is challenging due to its size and high rate of contraction, however advances in pre-clinical imaging now make this achievable. Furthermore, rapid development of a range of molecular probes for use in a number of imaging modalities allows more detailed *in vivo* analysis of processes including inflammation and fibrosis. Here we will demonstrate how we are using the Edinburgh Preclinical Imaging (EPI) facilities, including magnetic resonance imaging (MRI), high resolution ultrasound and fluorescence molecular tomography (FMT), to permit assessment of myocardial injury, infarct healing and changes in structure and function in the mouse after MI.

Work supported by Wellcome Trust, British Heart Foundation, British Heart Foundation Centre of Research Excellence

P38

Glucocorticoid receptor deficiency in cardiomyocytes results in cardiac fibrosis in adult mice.

R.V. Richardson, E.A. Rog-Zielinska, A.J.W. Thomson, C.M. Moran, C.J. Kenyon , G.A. Gray, K.E. Chapman.

Centre for Cardiovascular Science, The University of Edinburgh, The Queen's Medical Research Institute, Edinburgh, EH16 4TJ, UK

Variation in the glucocorticoid receptor (GR) gene associates with relative glucocorticoid resistance, hypertension and increased cardiovascular disease risk in humans. To investigate the contribution of cardiac GR to this phenotype we have characterised adult male mice with cardiomyocyte and vascular smooth muscle deletion of GR (SMGRKO) and have found left ventricular function to be impaired.

SMGRKO mice, generated by crossing GR "floxed" mice (congenic on C57BL/6J) with SM22 α -Cre mice, have reduced cardiac GR protein and mRNA levels (by 52% and 57%, respectively), compared to Cre-negative littermate controls.

The Visualsonics Vevo 770 High-Resolution Ultrasound *In Vivo* Micro-Imaging System was used to assess cardiac function at 10 weeks of age. Mitral valve Doppler showed a detrimental increase in the myocardial performance index (MPI), a marker of combined systolic and diastolic function, in SMGRKO mice. This was primarily due to greater isovolumetric contraction time (Control:12.9 \pm 0.8ms, SMGRKO:15.5 \pm 0.6ms, p <0.05) indicating impairment of the initial left ventricular contractile phase.

Heart weight (% body weight) is increased in SMGRKO mice (Control:0.5 \pm 0.02%, SMGRKO:0.55 \pm 0.01%, p <0.05) and they have elevated levels of cardiac mRNA encoding myosin heavy chain- β (Control:100 \pm 9%, SMGRKO:151 \pm 16%, p <0.05), mineralocorticoid receptor [MR (Control:100 \pm 14%, SMGRKO:151 \pm 19%, p <0.05)] and pro-fibrotic factors (collagen, TGF- β 1, CTGF). Cardiac expression of Ca²⁺ handling genes was unaltered. Histopathology shows fibrosis and a trend for increased cardiomyocyte cross-sectional area in the left ventricle of SMGRKO mice, suggestive of cardiomyocyte hypertrophy and pathological remodelling despite normal blood pressure.

These data demonstrate that cardiomyocyte/smooth muscle GR deficiency causes pathological changes in the left ventricle resulting in impairment of isovolumetric contraction in 10 week old mice. The findings support a role for cardiomyocyte GR in determination of cardiovascular disease risk.

P39

Effects of bs906, anHSP20-PDE4 disruptor, on hypertrophic remodelling *in vivo*

Tamara P. Martin¹, Susan Currie², George Baillie¹

1: *Institute of Medical, Veterinary and Life Sciences, University of Glasgow*

2: *Strathclyde Institute of Pharmacy and Biomedical Sciences, University of Strathclyde*

Heat shock protein 20 (HSP20) is a small protein constitutively expressed at high levels in skeletal, cardiac and vascular smooth muscle. HSP20 has been shown to exert cardioprotective effects which are dependent upon effects of HSP20 phosphorylation at Serine 16 by protein kinase A (PKA). In resting cells, HSP20 is kept inactive and unphosphorylated by association with PDE4 enzymes that dampen PKA activity in the vicinity of HSP20. Although pharmacological ablation of PDE4 activity results in hyperphosphorylation of HSP20, PDE4 inhibitors cannot be used clinically due to side effects that limit maximally tolerated doses. Previously, HSP20 was found to associate with the E⁴⁶⁸-K⁴⁹² region of PDE4D5 and this novel peptide was able to reverse isoprenaline induced neonatal cardiomyocyte hypertrophy [1]. Here we describe the anti-hypertrophic capacity of a novel cell permeable E⁴⁶⁸-K⁴⁹² peptide (bs906) disruptor of the HSP20-PDE4 complex *in vivo*. A minimally invasive transverse aortic banding (MTAB) mouse model was used to induce left ventricular (LV) hypertrophy [2]. Following MTAB surgery animals were dosed with either bs906 or a control scrambled peptide at 10mg/kg/week for 4 weeks. Heart weight:body weight ratios were significantly increased in MTAB+scrambled peptide compared to sham+scrambled peptide animals (6.0±0.6 cf. 4.7±0.21, n≥3, p<0.01), and LV contractility (% fractional shortening) was significantly depressed in MTAB+scrambled peptide compared to sham+scrambled peptide animals (29.2±2.2 cf. 46.43±5.1, n=5, p<0.001). Following treatment with bs906, heart weight:body weight ratios were significantly decreased in MTAB animals (4.9±0.2 cf. 6.0±0.6, n≥3, p<0.05, MTAB+ bs906 and MTAB+scrambled, respectively, and 4.9±0.2 cf. 4.8±0.1, n≥3, p>0.05, MTAB+bs906 and sham+bs906, respectively). LV contractile depression observed in MTAB animals was also reversed following bs906 treatment (38.5±2.5 cf. 29.2±2.2, p<0.5, n=5, MTAB+bs906 and MTAB+scrambled peptide, respectively, and 38.5±2.5 cf. 40.4±1.3, p>0.05 MTAB+bs906 and sham+bs906, % fractional shortening respectively).

Collectively, these initial results suggest that disrupting the HSP20-PDE4 complex using bs906 is an attractive strategy for reversing cardiac hypertrophy.

1. Sin, Y.Y., et al., (2011). Disruption of the cyclic AMP phosphodiesterase-4 – HSP20 complex attenuates the β-agonist induced hypertrophic response in cardiomyocytes. *J. Mol. Cell Card.*, 50(5):p872-883.

2. Martin T.P., et al., (2012). Surgical optimisation and characterisation of a minimally invasive aortic banding procedure to induce cardiac hypertrophy in mice. *Exp. Phys.* 97(7):p822-832

P40

The Role of Intermedin in modulating functional changes associated with Pulmonary Hypertension

M Campbell, MP Corr, MT Harbinson, D Holmes, D Bell

School of Medicine, Dentistry and Biomedical Sciences, Queen's University Belfast, Northern Ireland, UK.

Introduction: Pulmonary hypertension (PH) is a condition of elevated pulmonary arterial pressures as a result of vascular remodelling, driven by inappropriate pulmonary cell turnover, in the presence of chronic vasoconstriction. Current therapies target key pathological mediators, such as endothelin-1 (ET-1), but mortality rates remain high, suggesting other influential biochemical pathways have been overlooked. The novel peptide Intermedin (IMD) is a potent pulmonary vasodilator which acts via receptor complexes consisting of the calcitonin receptor-like receptor (CRLR) and various receptor-activity modifying proteins (RAMP). IMD is cytoprotective in several organs while the related peptide Adrenomedullin (AM) negatively regulates key pathophysiological processes in PH including cell proliferation and pulmonary smooth muscle cell (PSM) migration.

Aims: (i) To characterise distribution of IMD, AM and their receptor components across human pulmonary cell types and to develop a cell-culture model of PH. (ii) to assess the effect of simulated hypertension (\pm IMD) on PSM viability and on the cell transcriptome. (iii) to explore IMD's effect on PSM migration.

Methods: Primary human pulmonary macrovascular (PEC) and microvascular (PMVEC) endothelial cells as well as fibroblasts (PF) and PSM were cultured under normal conditions. Peptide and receptor expression at protein level were measured by semi-quantitative immunofluorescence and western blot. Gene expression was quantified by qRT-PCR. The Flexcell® apparatus was used to simulate hypertension by applying pulsatile mechanical strain to PSM. Cell viability was measured by trypan blue assay. Platelet-derived growth factor (PDGF-BB) was used as a chemo-attractant in the Dunn Chemotaxis Chamber.

Results: IMD mRNA and protein were most highly expressed in PMVEC while AM was most abundant in PSM. CRLR and RAMP1-3 were present in all cell types although CRLR was detected at a lower level than the RAMP proteins. RAMP2 was the predominant RAMP across all cell types studied. ET-1 mRNA expression was transiently up-regulated after 48 h (19-fold; $P < 0.0001$) and IMD mRNA doubled ($P < 0.01$) after 72 h of simulated hypertension. Significant up-regulation of receptor components was also observed. IMD 10^{-10} mol.L⁻¹ improved PSM viability during simulated hypertension ($P < 0.01$ vs. control); while IMD 10^{-9} mol.L⁻¹ prevented PDGF-induced PSM migration.

Conclusion: This study is the first to characterise the expression of these peptides and receptors across human pulmonary cells; variations in IMD and receptor distribution suggest possible paracrine signalling mechanisms. The PH model developed is validated both by highly-upregulated ET-1 expression and reduced viable cell numbers. Improvement in both PSM and PMVEC viability with IMD may be of benefit in PH by preventing the emergence of hyper-proliferative apoptosis-resistant cells.

P41

Finding potential anti-diabetic compounds from *Allophylus cominia* Sw.

Dima Semaan¹, Edward Rowan¹, Alexander Gray¹, A.L.Harvey¹, B.Furman¹, J.Sanchez², E. Marrero², J. O. Igoli¹, L.Young¹, C.Clements¹

1. University of Strathclyde, Glasgow, UK

2. Censa, La Habana, Cuba

Type 2 Diabetes Mellitus (T2-DM) commonly associated with obesity (diabesity) leads to an increase in the risk of cardiovascular problems such as systolic or diastolic hypertension, atherosclerosis (coronary heart disease). Hyper-insulinaemia caused by insulin resistance is the important link between T2-DM and cardiovascular diseases. This project strives to find potential anti-diabetic compounds from a Cuban plant *Allophylus cominia* (L.) Sw (leaves) that increase glucose uptake in peripheral tissues (muscle and adipose tissue), limit glycogen synthesis and lead to glucose homeostasis which correlates directly with the severity of (T2-DM) induced hypertension.

Based on ethno-botanical information collected from diabetic patients in Cuba, *A.cominia* has been used for the treatment of T2-DM. Extracts of *A.cominia* were tested to demonstrate their ability to inhibit the activity of two enzymes: DPPIV and PTP1B. Crude extracts of *A.cominia* have produced a potent inhibition of the PTP1B enzyme which plays a role in inhibiting signalling downstream of the insulin and leptin receptors. On a 2-NBDG glucose uptake assay using HepG2 cells, 3T3 fibroblasts and differentiated 3T3-L1 adipocytes, these extracts enhanced insulin activity by increasing glucose uptake, thus decreasing insulin secretion by β -cells, therefore decreasing the potential risk of cardiovascular diseases. Chemical characterization of the extracts was carried out using phytochemical methods. Fatty acids, tannins, Phaeophytins (A and B), and a mixture of flavonoids were detected. The identified flavonoids were: Mearnsitrin, Quercitrin, Quercetin-3-alloside, and Naringenin-7-glucoside. Some of these compounds have been reported in literature as potent hypoglycaemic agents. These compounds may be responsible for the pharmacological effects observed in experimental diabetic models. Further separation techniques will be employed to purify the mixtures of compounds remaining in order to profile the active constituents and attempt to verify their individual mechanism(s) of action.

P42

Pharmacological Analysis of Sympathetically-Mediated Constriction in Mouse Tail Artery.

Claire Stevenson¹, Craig Daly¹, Elspeth McLachlan², Ian McGrath¹

1: Autonomic Physiology Unit, School of Life Sciences, University of Glasgow

2: Neuroscience Research Australia, Randwick, NSW, Australia

Neurovascular transmission in the tail artery of normal mice can be defined using pharmacological antagonists, as has been done for the rat. Perivascular stimulation of rat tail artery evokes contraction mediated by adenosine triphosphate (ATP) and noradrenaline (Sneddon and Burnstock, 1984) with contraction mediated largely by α_1 - and α_2 -adrenoceptors (AR), probably acting synergistically (Brock et al., 1997; Yeoh et al., 2004). The post-junctional α_2 -AR-mediated effects are more readily shown distally (Medgett, 1985). Capsaicin-sensitive afferent nerves are rare around the rat tail artery (Li and Duckles, 1993) but may be present in the mouse. Here we report a pharmacological analysis of neurovascular transmission in proximal and distal mouse tail artery.

Male C57Bl mice (4-6 months) were killed with CO₂. Ring segments of the tail artery 2mm long were prepared from proximal (2cm) and distal (5cm) sites. Vessels were mounted on a wire myograph in oxygenated physiological saline at 37°C. Frequency response curves (FRC) to maximal stimuli were constructed without and with pretreatment with 1 μ m capsaicin (depletes calcitonin gene-related peptide from afferent nerves) (0.5 Hz – 8 Hz; 20 pulses; 0.3 ms pulse width; 20 V) and in the presence of various combinations of 100 nM prazosin (α_1 -AR antagonist), 100 nM rauwolscine (α_2 -AR antagonist), and 1 mM suramin (P2X receptor antagonist). Paired and unpaired t-tests were carried out as appropriate, with P<0.05 taken as significant.

Perivascular stimulation resulted in production of a two component response that consisted of an initial fast contraction followed by a sustained contraction and was not affected by capsaicin. At both locations, the initial component was reduced by each antagonist individually (P<0.05), with prazosin having a greater effect than rauwolscine at 8 Hz. The second component was reduced by rauwolscine proximally (P<0.05) but by both rauwolscine and prazosin distally (P<0.05). Rauwolscine reduced the response to a greater degree than the other antagonists at 0.5 Hz, and the second component was reduced more by rauwolscine than prazosin (P<0.05; n=7). Suramin had variable effects, potentiating responses in 4 out of 7 proximal segments and 2 out of 7 distal segments.

The results show that both post-junctional α_1 - and α_2 -ARs are involved in nerve-evoked contraction of mouse tail artery. Contractions mediated by α_2 -ARs dominate at low stimulation frequencies similar to natural tonic nerve firing, especially in the distal artery. Unlike the rat tail artery, the involvement of P2X receptors in nerve evoked contraction is unclear. Arteries from mice that lack α_1 -ARs will be used to clarify the roles of α_2 -ARs and P2X receptors.

References:

1. Sneddon P. & Burnstock G. (1984) *Eur J Pharmacol.* 106: 149-152.
2. Brock J. A., McLachlan E. M. & Rayner S. E. (1997) *Br J Pharmacol.* 120: 1513-1521.
3. Yeoh M., McLachlan E. M. & Brock J. A. (2004) *J Physiol.* 561: 583-596.
4. Medgett I. C. (1985) *Eur J Pharmacol.* 108 : 281-287.
5. Li Y. & Duckles S. P. (1993) *Eur J Pharmacol.* 236 : 373-378.

P43

Pulmonary Exposure to Diesel Exhaust Particulate Inhibits the Cytoprotective Mechanisms of the Heart

Holly Stott¹, Sarah Robertson¹, Ashleigh L Thomson¹, Catherine Shaw¹, Paddy Hadoke¹, Mark Miller¹ & Gillian A Gray¹,

1: The Centre of Cardiovascular Research, The Queens Medical Research Institute, The University of Edinburgh

Introduction- Exposure to particulate matter (PM) is associated with various cardiovascular diseases. In previous studies from this lab, instillation of diesel exhaust particulate (DEP, rich in PM) into the lung was shown to prime the heart for increased myocardial infarction injury following ischemia and reperfusion (I/R), but the underlying mechanisms are not fully understood. In vivo and in vitro functional studies support the hypothesis that the sympathetic nervous system (SNS) plays a vital role; potentially secondary to activation of a pulmonary reflex involving transient receptor potential vanilloid 1 (TRPV1) receptors. This study aimed to investigate the extent to which the heart was injured prior to I/R and whether SNS or TRPV1 blockade could prevent this.

Methods- A sonicated suspension of DEP (0.5 mg) or saline was instilled into the lungs of Wistar rats alone or in conjunction with a TRPV1 antagonist (AM9810, 10 mg/kg) to block sensory neurons in the lung. In parallel experiments a β 1 adrenoreceptor antagonist (metoprolol, 10mg/kg) was administered intraperitoneally to block SNS activation. The hearts were removed 6 hours later, fixed in formaldehyde and embedded in paraffin. Following tissue processing, 5 μ m sections were prepared for examination on a cellular level. Haematoxylin and Eosin staining allowed assessment of tissue structure. Immunohistochemistry was utilised to assess levels of apoptosis (TUNEL assay) and levels of oxidant stress induced DNA damage (8-OHdG antibody).

Results- Hearts from rats exposed to DEP had an increased incidence of apoptotic cells in the left ventricle ($P < 0.01$); this was prevented in the hearts from drug treated animals (Metoprolol and AM9810). Assessment of levels of oxidative DNA damage using the 8-OHdG antibody were inconclusive.

Conclusion- It is proposed that the cytoprotective mechanisms in the heart are impaired by activation of a pulmonary sensory reflex SNS by pulmonary DEP. resulting in direct damage to the myocardium before induction of I/R injury.

HS is supported by a BHF Centre for Research Excellence 4 year PhD award

P44

Differences in the signalling mechanisms underlying UTP-evoked vasoconstriction of pulmonary and systemic-like arteries

Nawazish-i-Husain Syed*, Asrin Tengah, Siti Tajidah Abdul Talip, Siti Nur Basirah Bujang and Charles Kennedy

Strathclyde Institute of Pharmacy and Biomedical Sciences, University of Strathclyde, 161 Cathedral Street, Glasgow G4 0RE, United Kingdom.

P2Y receptors are G protein-coupled receptors that are activated by the endogenous nucleotide, UTP. In the vascular system P2Y receptors located on arterial smooth muscle cells mediate vasoconstriction (Chootip *et al.*, 2002). Previously we showed that Ca^{2+} influx via $Ca_v1.2$ ion channels contributes to the UTP-evoked contraction of rat intrapulmonary arteries (rIPA) (Mitchell *et al.*, 2012). The aim here was to characterise and compare the contribution of Ca^{2+} release and influx, rho kinase and protein kinase C in rIPA, a low pressure, low resistance vessel, and rat tail artery (rTA), a resistance-like, systemic artery.

5 mm rings of rIPA and rTA were dissected from male Sprague-Dawley rats (200-250g). The endothelium was removed and rings were mounted under isometric conditions in 1ml baths at 37°C and a resting tension of 0.5-0.75g. Tension was recorded by Grass FT03 transducers connected to a Powerlab/4e system (AD Instruments). Contractions were elicited by adding UTP (300 μ M-rIPA; 1 mM-rTA) to the bath. Data were analysed using Student's paired and unpaired t tests. Values of $P < 0.05$ were considered to be statistically significant.

UTP evoked slowly developing contractions in both tissues, which peaked within 2-3 min. Thapsigargin (1 μ M) depressed significantly contractions by 30-40% (rIPA- $P < 0.001$, $n=8$; rTA- $P < 0.05$, $n=4$), but ryanodine was ineffective ($n=5$). The rho kinase inhibitor, Y27632 (10 μ M) significantly reduced the peak amplitude of contractions by about 20% in rIPA ($P < 0.01$, $n=5$) and by more than 80% in rTA ($P < 0.01$, $n=4$) and the inhibition was significantly greater in rTA ($P < 0.001$). The protein kinase C inhibitor, GF109203X (10 μ M) also significantly reduced the peak amplitude in rIPA by over 20% ($P < 0.01$, $n=7$) and by around 40% in rTA ($P < 0.001$, $n=5$). Inhibition was again significantly greater in rTA ($P < 0.05$). In rIPA, adding Y27632 (10 μ M), GF109203X (10 μ M), thapsigargin (1 μ M) and nifedipine (1 μ M) together abolished the UTP response ($n=4$). In rTA nifedipine (1 μ M) significantly reduced the amplitude of UTP response by about 60% ($P < 0.01$, $n=6$). Furthermore, contractions were abolished by Y27632 (10 μ M) plus thapsigargin (1 μ M, $n=5$), GF109203X (10 μ M, $n=4$) or nifedipine (1 μ M, $n=4$). Adding thapsigargin (1 μ M), GF109203X (10 μ M) and nifedipine (1 μ M) together abolished UTP-evoked contractions ($n=4$).

These results indicate that Ca^{2+} release from the sarcoplasmic reticulum and Ca^{2+} influx through $Ca_v1.2$ channels, contribute to UTP-evoked vasoconstriction of rIPA and rTA. Rho kinase and protein kinase C are also involved, but more so in rTA. Thus the relative importance of signalling components differs in pulmonary compared with systemic arteries.

Chootip K *et al.*, (2002). *Br. J. Pharmacol.*, **137**, 637-646.

Mitchell C *et al.*, (2012). *Br. J. Pharmacol.*, **166**, 1503-1512.

P45

A critical role for MAP kinase phosphatase-2 in the completion of vascular smooth muscle cell cytokinesis

Emma Torrance¹, Louise Collins³, Eileen Miller², Gwyn Gould³, Patrick Hadoke², Robin Plevin¹.

1 Strathclyde Institute of Pharmacy and Biomedical Science, University of Strathclyde.

2 The Queen's Medical Research Institute, University of Edinburgh.

3 Institute of Molecular Cell and Systems Biology, University of Glasgow.

Major cardiovascular conditions are associated with a pathophysiological modification within the blood vessel, driven by vascular smooth muscle cell (VSMC) hyperproliferation (Schiffrin, 2010). Upon initial insult, VSMCs migrate and proliferate into the intimal layer of the vessel resulting in reduced lumen area, restricting blood flow and subsequently increasing the potential risk for myocardial infarction and stroke. It is well established that MAP kinases play a commanding role in the induction of the VSMC hyperproliferative phenotype (Schad *et al.*, 2011). Regulatory mitogen-activated protein kinase phosphatase-2 (MKP-2) is a type 1 nuclear phosphatase with the ability to dephosphorylate and ultimately inactivate MAP kinases ERK and JNK in vitro (Lawan *et al.*, 2012). Therefore, MKP-2 may be a novel therapeutic target in cardiovascular disease. In order to examine this further, we examined the role of MKP-2 in the regulation of MAP kinase phosphorylation, cell proliferation, and cell cycle progression in mouse aortic smooth muscle cells (MASMCs) derived from a novel MKP-2 (DUSP-4) deletion mouse. Contrary to current literature, serum and PDGF stimulated MASMC ERK phosphorylation was not different in MKP-2^{-/-} compared with wild type. Interestingly however, cellular proliferation rates were significantly reduced in MKP-2^{-/-} MASMCs and further cell cycle analysis revealed a significant block in G2/M phase transition in MKP-2 deficient cells, compared with wild-type. Further investigation utilising time-lapse microscopy noted a delay in cytokinesis and failure in abscission which consequently resulted in an increased number of multinucleate smooth muscle cells in the MKP-2^{-/-} cohort. This was correlated with a reduction in activity of the late mitotic kinase, Aurora B with no significant difference in Aurora B endogenous protein levels. Furthermore, catalytically-inactive MKP-2 adenovirus (Adv.MKP-2-CI), as a gain of function tool lacking phosphatase activity, reversed the mitotic accumulation in MKP-2^{-/-} MASMCs suggesting MKP-2 action not reliant upon its phosphatase activity. Collectively, these data suggest a novel role for MKP-2 in mouse aortic smooth muscle cell proliferation, providing novel insights into the understanding of MKP-2 in the completion of cytokinesis. Hence modifying MKP-2 expression or function may represent a new approach in reducing VSMC hyperproliferation in vascular disease states.

Lawan *et al.*, (2012) *Biochem Soc Trans.* 40(1):235-9

Schad *et al.*, (2011) *Vasc Cell.* 19(3):21

Schiffrin EL (2010). *J Cell Mol Med* 14(5): 1018-1029

P46

Canine adenovirus as a novel gene delivery vector for experimental stroke studies

Josie van Kralingen¹, Lorraine M. Work¹

1: Institute of Cardiovascular and Medical Sciences, College of Medical, Veterinary and Life Sciences, University of Glasgow, Scotland, UK

Efficient gene delivery to the brain remains a limiting factor for its application for neurodegenerative disorders such as stroke. Canine adenovirus-2 (CAV2) has been shown to result in significant transduction of neurons following stereotactic delivery with marked retrograde transport from the injection site¹. This has led to the proposal that CAV2 may be a powerful molecular tool for the study of many neurodegenerative diseases including stroke. Ischaemia has been shown to induce a down-regulation in ZEB1 mRNA and protein levels in cortical neurons² and ZEB1 in pancreatic and breast human cancer cell lines causes a reduction in the expression of the primary receptor for CAV2, the coxsackie and adenovirus receptor (CAR) and therefore adenovirus uptake³. The aim of this study was to determine if efficient gene delivery remained feasible after cerebral ischaemia/reperfusion or whether the alterations in CAR expression associated with alterations in ZEB would limit the use of this novel gene delivery vector in the therapeutic setting of stroke.

ZEB1 and CAR expression was quantified in cerebral endothelial (GPNT) and neuronal (B50) cell lines following hypoxic challenge using qRT-PCR. A trend towards an increase in ZEB1 mRNA expression was observed in GPNT and B50 cells following hypoxia (without re-oxygenation). CAR expression, however, was highly variable in both cell types. *In vivo*, relative expression of ZEB1 and CAR was quantified from RNA of spontaneously hypertensive stroke prone rats (SHRSP) from the brain which was harvested 1 day post-transient middle cerebral artery occlusion (tMCAO). ZEB1 expression was increased in infarct tissue, with a corresponding decrease in CAR expression. However, CAR expression was decreased in peri-infarct tissue independent of an increase in ZEB1 expression. Levels of transduction following CAV2 delivery were assessed 7 days post-virus delivery – 3×10^9 vp CAV-GFP were delivered stereotactically into the cortex either 4 days before or 1 day post-tMCAO in SHRSP. Immunohistochemistry using specific α -GFP (reporter gene) and α -NeuN (neurons) antibodies was performed to determine levels of transgene expression from groups administered CAV-GFP and to determine if expression was altered post-tMCAO. The total area of transduction was consistently reduced following post-tMCAO CAV-2 delivery as compared to pre-tMCAO CAV2 delivery. Specific transduction of neurons by CAV2 was observed.

These studies have important implications for CAV2 mediated gene delivery as a novel therapeutic approach to promote neurorepair/recovery when administered post-experimental stroke.

¹Soudais *et al* (2001) FASEB J **15** 2283-2285

²Bui *et al* (2009) PLoS One **4** e4373

³Lacher *et al* (2011) Mol Cancer **10** e91

P47

Pharmacological Effects of Gallic Acid from *Benincasa hispida* Prepared with Different Extraction Techniques: A Preliminary Quantitative Analysis

¹Wan Rosli, W. I, ¹Fatariah Z. and ²Tg. Zulkhairuazha T. Y.

1: Nutrition Programme, School of Health Sciences, Universiti Sains Malaysia, 16150 Kubang Kerian, Kelantan, Malaysia.

2: Therapeutic Drug Monitoring, Pharmacy Department, Hospital Universiti Sains Malaysia, 16150 Kubang Kerian, Kelantan, Malaysia.

ABSTRACT

Ash gourd (AG) or winter melon (*Benincasa hispida*) is traditionally claimed useful in treating asthma, cough, diabetes, haemoptysis and hemorrhages from internal organs, epilepsy, fever and myocardium protection. One of the major phenolic acids presented in natural product is gallic acid which was reported to exhibit significant protective effect on cardiac marker enzymes. The aim of the study was to investigate the effect of different extraction techniques on the concentration of gallic acid in AG. Ash gourd sample was prepared with three different extraction techniques namely (i) fresh extract (FE), ii) low heating (LH) and iii) drying and heating (DH). The gallic acid has been detected and quantified using high performance liquid chromatography (HPLC) coupled with UV-Vis detector. Amount of gallic acid detected in FE, LH and DH were 0.036 mg/100g, 0.050 mg/100g and 0.272 mg/100g, respectively. The limits of detection was 0.75 µg/ml while the limit of quantification and recovery were 2.50 µg/ml and 95.53%, respectively. In summary, the present preliminary study demonstrated that gallic acid was occurred at the highest concentration in AG extracted using drying and heating, followed by low heating and fresh extracts. The gallic acid from Bh extracts will be further investigated on its ability to protect myocardial infarction *in vivo*.

P48

Cardiovascular phenotyping of mice with targeted 11 β -hydroxysteroid dehydrogenase type 1 deletion

Christopher I White¹, Adrian Thomson¹, Xiaofeng Zhao¹, Carmel Moran¹, Karen E Chapman¹ & Gillian A Gray¹

1: BHF/University Centre for Cardiovascular Science, Queen's Medical Research Institute, University of Edinburgh, 47 Little France Crescent, Edinburgh, EH16 4TJ.

11 β -hydroxysteroid dehydrogenase type 1 (11 β -HSD1), responsible for intracellular regeneration of corticosteroids, is expressed widely in the cardiovascular system. This study aimed to determine the cardiovascular phenotype of mice in which 11 β -HSD1 was specifically deleted in cardiomyocytes and vascular smooth muscle cells by Cre-mediated recombination (Hsd11b1^{fl/fl}Sm22 α -Cre⁺).

Western blotting and qRT-PCR confirmed loss of 11 β -HSD1 only in cardiomyocytes and vascular smooth muscle cells of Hsd11b1^{fl/fl}Sm22 α -Cre⁺ mice. Blood pressure, assessed by tail plesytmography, was similar in Hsd11b1^{fl/fl}Sm22 α -Cre⁺ and control (Hsd11b1^{fl/fl}Sm22 α -Cre⁻) littermates. High frequency ultrasound demonstrated that cardiac structure and systolic function were similar in both groups at 6, 10, 20 and 35 weeks of age, with comparable end systolic and diastolic areas and ejection fractions. Consistent with this, post-mortem heart weight to body weight ratio was similar in both groups. Mitral valve pulsed-wave Doppler ultrasound showed that E/A wave ratios were similar in Hsd11b1^{fl/fl}Sm22 α -Cre⁺ and controls. However, E wave deceleration was reduced, and deceleration time (MVDT) increased, in Hsd11b1^{fl/fl}Sm22 α -Cre⁺ mice versus controls, suggesting mild diastolic dysfunction due to reduced compliance or relaxation deficit. This could not be accounted for by changes in myocardial collagen content. However, histological analysis of the mitral valves demonstrated a thickening of the posterior leaflets in Hsd11b1^{fl/fl}Sm22 α -Cre⁺ mice compared to controls, indicative of mitral valve stenosis. This may give rise to the changes in E wave deceleration and MVDT observed by Doppler ultrasound. qRT-PCR revealed that sarcoplasmic reticulum Ca²⁺-ATPase (SERCA2a) expression was reduced in Hsd11b1^{fl/fl}Sm22 α -Cre⁺ mice compared to controls. Furthermore, cardiomyocytes isolated from global 11 β -HSD1 deficient mice displayed a reduced rate of spontaneous contraction consistent with SERCA2a deficiency.

These data demonstrate that cardiovascular 11 β -HSD1 deficiency results in preserved systolic function with mild diastolic dysfunction in vivo. Altered Ca²⁺ handling within cardiomyocytes and alterations in mitral valve morphology may impair relaxation and contribute to development of this phenotype.

P49

The miR-143/145 cluster is dysregulated during progression of vein graft and in-stent neointima formation but genetic deletion in mice does not influence lesion formation.

Katie White¹, Robert A McDonald¹, Hollie C Robinson¹, Keith E Robertson¹, Junxi Wu², Ruifang Lu¹, Jia Hu³, Simon Kennedy¹, Cecile Carvajal¹, Sarah J George⁴, Sheila Francis⁵, Keith Oldroyd¹, Roger M Wadsworth², Eva van Rooij⁶, Song Wan³, Andrew H Baker¹

¹Institute of Cardiovascular and Medical Sciences, University of Glasgow, Glasgow.

²Strathclyde Institute of Pharmacy and Biomedical Sciences, University of Strathclyde, Glasgow. ³Division of Cardiothoracic Surgery, Prince of Wales Hospital, The Chinese University of Hong Kong, Hong Kong. ⁴Bristol Heart Institute, School of Clinical Sciences, Bristol Royal Infirmary, Upper Maudlin Street, Bristol. ⁵Department of Cardiovascular Science, University of Sheffield, Beech Hill Road, Sheffield. ⁶miRagen Therapeutics Inc., 6200 Lookout Road, Boulder, CO 80301, USA.

Background: The microRNA cluster miR-143/145 is abundantly expressed in vascular smooth muscle cells and is thought to have an important role in maintaining their quiescent, contractile phenotype. In several small animal models of acute vascular injury, a decrease in miR-143/145 expression has been reported and implicated in pathogenic remodelling. Therefore we investigated whether miR-143/145 is also altered during vascular remodelling associated with vein grafting and in-stent restenosis.

Methods and Results: In a porcine model of in-stent restenosis, qRT-PCR demonstrated that miR-143/145 expression was selectively down-regulated in stented vessels. However, *in situ* hybridisation revealed high levels of expression in the developing neointima. In mouse, porcine and human models of vein graft neointima formation miR-143/145 expression was also significantly lower in homogenates from whole vein grafts compared to ungrafted control veins. However, high levels were observed in the neointima. Comparison of vein grafts from wild-type and miR-145 knockout mice showed no difference in the size or cellular composition of neointimas analysed 28 days post engraftment. In addition, over-expression or knockdown of miR-143 or miR-145 in primary human saphenous vein smooth muscle cells had no effect on cell proliferation or migration.

Conclusions: miR-143/145 expression in vascular remodelling is dynamic. Following stenting or vein grafting, expression is decreased in whole vessel homogenates, but high levels are present in neointimal cells. Genetic ablation of miR-145 does not affect neointima formation in a mouse model of vein grafting and pharmacological modulation of miR-143/145 expression *in vitro* does not affect smooth muscle cell proliferation or migration. These findings suggest that the role of miR-143 and miR-145 in vascular remodelling remains to be fully defined.

P50

Glucocorticoids are important for maturation and development of the zebrafish embryo cardiovascular system.

K.S. Wilson¹, G. Matrone, C.S.Tucker, C.J.Kenyon, J.J.Mullins,
P.W.F. Hadoke, M.A. Denvir

1: BHF centre of Cardiovascular Science, The University of Edinburgh, The Queen's Medical Research Institute, Edinburgh

The relationship between adverse fetal environment and excess cardiovascular risk in adult life is well established in clinical observational studies and has been modelled in rodents using fetal exposure to glucocorticoids (GC). The underlying mechanisms are poorly understood, however early exposure to GCs could directly affect the structure and function of the developing cardiovascular system. The zebrafish embryo is a potentially useful model to explore this hypothesis.

We assessed the suitability of the zebrafish embryo as a model for GC manipulation by targeting the activity of the GC receptor (GR) pharmacologically and molecularly. Zebrafish embryos at the 2-cell stage were exposed either to the GR agonist dexamethasone [100uM], the GR antagonist RU486 [10uM] or microinjected with a morpholino to produce a targeted gene expression knock down (40% reduction in mRNA). Over the course of the following 120 hour various cardiovascular structural and functional assessments were carried out along with gene expression analysis using qRT-PCR.

Reduced GR activity, in both RU486 and morpholino groups, resulted in significantly smaller hearts, compared to controls ($67 \pm 3.5 \mu\text{m}$ and $75 \pm 2.4 \mu\text{m}$ respectively compared to controls $90.2 \pm 0.8 \mu\text{m}$ $p < 0.05$) with impaired cardiac function (heart rate and ejection fraction). Isolated hearts showed an immature cardiac phenotype with reduced cardiomyocyte striation pattern and smaller less dense nuclei. Gene expression analysis of growth factors and cardiac structural proteins suggested that these hearts were developmentally less mature than controls (vmhc expression $p < 0.001$ at 72hpf and $p < 0.05$ at 120hpf).

Enhanced GR activity in the form of dexamethasone incubation resulted in larger hearts ($107.2 \pm 4.5 \mu\text{m}$ compared to controls $90.2 \pm 0.8 \mu\text{m}$ $p = 0.048$) with increased ejection fraction and significantly fewer cardiomyocytes compared to controls ($p = 0.034$) suggesting possible cardiac hypertrophy. There was no difference in structural protein gene expression compared to controls.

Manipulation with GR agonist, antagonist and morpholino resulted in altered blood vessel appearance, a decrease in branching was observed in dexamethasone treated embryos, this coupled with a reduced level of known pro-angiogenic factors (reduced vegfaa expression $p = 0.054$) suggests a possible role of GCs in endothelial cell migration and vasculogenesis.

These findings suggest a key role for GCs and the GR in development of the cardiovascular system in the zebrafish.

P51

A protective role for FGF23 in local defence against disrupted arterial wall integrity?

Dongxing Zhu¹, Neil C W Mackenzie¹, Jose Luis Millan²; Colin Farquharson¹, Vicky E MacRae¹

1: The Roslin Institute and Royal (Dick) School of Veterinary Studies, The University of Edinburgh, Easter Bush, Roslin, Midlothian, EH25 9RG, Scotland, UK

2: Sanford Children's Health Research Center, Sanford-Burnham Medical Research Institute, La Jolla, CA 92037, USA

Abstract

Increasing interest is focusing on the role of the FGF-23/Klotho axis in mediating vascular calcification. However, the underpinning mechanisms have yet to be fully elucidated. Murine VSMCs were cultured in calcifying medium for a 21d period. FGF-23 mRNA expression was significantly up-regulated by 7d (1.63 fold; $P < 0.001$), with a concomitant increase in protein expression. mRNA and protein expression of both FGFR1 and Klotho were confirmed. Increased FGF-23 and Klotho protein expression was also observed in the calcified media of *Enpp1*^{-/-} mouse aortic tissue. Reduced calcium deposition was observed in calcifying VSMCs cultured with recombinant FGF-23 (10ng/ml; 28.1% decrease; $P < 0.01$). Calcifying VSMCs treated with PD173074, an FGFR1 inhibitor, showed significantly increased calcification (50nM; 87.8% increase; $P < 0.001$). FGF-23 exposure induced phosphorylation of ERK1/2. Treatment with FGF-23 in combination with PD98059, an ERK1/2 inhibitor, significantly increased VSMC calcification (10 μ M; 41.3% increase; $P < 0.01$). FGF-23 may represent a novel therapeutic strategy for inhibiting vascular calcification.

